UNIVERSITY OF CALIFORNIA, SAN DIEGO

SAN DIEGO STATE UNIVERSITY

Microbes versus Fish: The Bioenergetics of Coral Reef Systems

A dissertation submitted in partial satisfaction of the requirements for the degree
Doctor of Philosophy

in

Biology

by

Tracey Shannon McDole

Committee in charge:

University of California, San Diego

Professor Farooq Azam
Professor Kaustuv Roy

San Diego State University

Professor Forest Rohwer, Chair
Professor David Lipson
Professor Jim Nulton
Professor Peter Salamon

2012

The Dissertation of Tracey Shannon McDole is approved, and is acceptable in quality and form for publication on microfilm and electronically:

_____

_____

_____

_____

_____

_____
Chair

University of California, San Diego
San Diego State University
2012

DEDICATION

I am grateful to my advisor, Forest Rohwer, who taught me that “you can’t do anything linearly – otherwise you’d be like old and grey before you got anything done”.

EPIGRAPH

The less inquisitive you are as you go along, the less trouble you are likely to find.

- *J.R.R. Tolkien*

TABLE OF CONTENTS

LIST OF FIGURES

LIST OF TABLES

ACKNOWLEDGEMENTS

Chapter 2, in full, is a reprint of the material as it has been published in PloS ONE. Tracey McDole, James Nulton, Katie Barott, Ben Felts, Carol Hand, Mark Hatay, Hochul Lee, Mark Nadon, Bajador Nosrat, Peter Salamon, Barbare Bailey, Stuart Sandin, Bernard Vargas-Angel, Merry Youle, Brial Zgliczynski, Rusty Brainard, and Forest Rohwer; 2012. The dissertation author was the primary investigator and author of this paper.

Chapter 3, in full, is a reprint of the material as it has been submitted to Proceedings of the Royal Society B: Biological Sciences. Tracey McDole, Brett Hilton, Juris Agrasis, James Nulton, Barbara Bailey, Bajador Nosrat, Chris Sullivan, Mark Hatay, Katie Barrott, Bernardo Vargas-Angel, Rusty Brainard, and Forest Rohwer. The dissertation author was the primary investigator of this paper.

VITA

2012 Doctor of Philosophy, University of California at San Diego and San Diego State University

2004-2005 Research Associate, Gen-Probe

2003 Research Assistant, California Toxicology Research Institute

2002 Bachelor of Science, Florida Institute of Technology

PUBLICATIONS

McDole, T, Hilton, B, Agrasis, J, Nulton, J, Bailey, B, Nosrat , B, Sullivan, C, Hatay, M, Barrott, K, Vargas-Angel, B, Brainard, RE, Rohwer, F (submitted) Microbial-mediated resilience on intermediately disturbed coral reefs.

McDole, T, Nulton, J, Barott, KL, Felts, B, Hand, C, Hatay, M, Lee, H, Nadon, MO, Nosrat, B, Salamon, P, Bailey, B, Sandin, SA, Vargas-Angel, B, Youle, M, Zgliczynski, BJ, Brainard, RE, Rohwer, F (2012) Assessing Coral Reefs on a Pacific-wide Scale Using the Microbialization Score. PLoS One 7:9 e43233.

Cassman, N, Prieto-Davó, A, Walsh, K, Gilva, GGZ, Angly, F, Akhter, S, Barott, K, Busch, J, **McDole, T**, Haggerty, M, Willner, D, Alarcon, D, Ulloa, O, DeLong, E, Dulith, B, Rohwer, F, Dinsdale, EA (2012) Oxygen minimum zones harbor novel viral communities with low diversity. Environ Microbiol doi:10.1111/j.1462-2920.2012.02891.

Willner, D, Furlan, M, Schmieder, R, Grasis, JA, Pridec, DT, Relmanc, DA, Angly, FE, **McDole, T**, Mariella, RP, Rohwer, F and Haynes, M (2010) Metagenomic detection of phage-encoded platelet-binding factors in the human oral cavity. PNAS doi: 10.1073/pnas.1000089107.

Angly FE, Willner, D, Prieto-Davó, A Edwards, R, Schmieder, R, Vega-Thurber, R, Antonopoulos, D, Barott, K, Cottrell, MT, Desnues, C, Dinsdale, EA, Furlan, M, Haynes, M, Henn, MR, Hu, Y, Kirchman, DL, **McDole, T**, McPherson, JD, Meyer, F, Miller, RM, Mundt, E, Naviaux, RK, Rodriguez-Mueller, B, Stevens, R, Wegley, L, Zhang, L, Zhu, B, Rohwer, F (2009) The GAAS Metagenomic Tool and Its Estimations of Viral and Microbial Average Genome Size in Four Major Biomes. PLoS Comput Biol 5(12): e1000593. doi:10.1371/journal.pcbi.1000593.

ABSTRACT OF THE DISSERTATION

Microbes versus Fish: The Bioenergetics of Coral Reef Systems

by

Tracey Shannon McDole

Doctor of Philosophy in Biology

University of California, San Diego, 2012
San Diego State University, 2012

Professor Forest Rohwer, Chair

Metabolic rate refers to the rate by which chemical energy is converted into biological energy and used for either maintenance of existing structure or production of new biomass. The Metabolic Theory of Ecology (MTE) predicts the metabolic rate of individual organisms based on the observation that most variation in an individual's metabolic rate can be explained by body size and temperature. The objective of this dissertation was to investigate the bioenergetics of coral reef systems using MTE. My hypothesis was that human activities alter the energy budget of the reef system, specifically by altering the allocation of metabolic energy between microbes and macrobes. I found that in reef systems, even a small increase in microbial biomass can result in substantial changes in whole system rates of energy and materials flux. By comparison, relatively large reductions in fish biomass, affect the system bioenergetics to a lesser degree. The percentage of the combined fish and microbial predicted metabolic rate that is microbial, a.k.a. the microbialization score, was used as a metric

for assessing and comparing reef health. My results demonstrated a strong positive correlation between reef microbialization scores and human impact. Regardless of oceanographic context, the microbialization score was a powerful metric for assessing the level of human impact a reef system is experiencing. The process of microbialization was further examined by assessing the effects of human activity on the relative roles of heterotrophic and autotrophic microbes. I found that shifts in microbial trophic structure change both the magnitude *and* efficiency of energy flow. Specifically, there was a significant increase in the ratio of autotrophic to heterotrophic microbes with human impact, which was also related to an increase in the mass specific energy requirements (W g^{-1}) of the microbial community. I am proposing that microbialization is actually a mechanism of reef resilience that dampens the effects of both overfishing and eutrophication. In conclusion, this research sheds new light on the effects that rising human impact has on the bioenergetics of coral reef systems and adds to our current understanding of the mechanism(s) that underlie reef system degradation.

CHAPTER 1

Body Size Allometry and Metabolic Theory of Ecology (MTE)

Introduction

Body size allometry refers to equations which describe the relationship between the mass of an organism and another of its characteristics (y) (1). In fact, the word “allometry”, is derived from the root words “allos” meaning “other” and “metron” or “measure”. These relationships typically take the form presented in Equation 1, where body size (W) and whatever characteristic y represents typically increase at different rates; the dependent variable y changes as some power of body size.

$$y = aW^b \qquad \text{Equation 1}$$

Traditionally, the data is logarithmically transformed (Equation 2) so that linear regression analysis can be performed.

$$\log y = \log a + b \log W \qquad \text{Equation 2}$$

Because a represents a taxon-specific normalization constant, $\log a$ is also a constant, so the new form of the equation is a straight line.

$$y = mx + b \qquad \text{Equation 3}$$

The change in the dependent characteristic y with the independent variable body size (W), is called the *scaling* of that characteristic to body size, represented as b in Equation 1. Therefore, b is called the scaling exponent. Scaling indicates that some

quality is being preserved while everything else changes. Of course, mathematics is only a means for *expressing* the laws that govern complex phenomenon and one of the most common gripes against body size allometry is that these equations sacrifice precision for generality. Allometric relationships between metabolic rate and body size underlie the foundation of Metabolic Theory of Ecology (MTE). As stated by James brown, one of the founders of MTE "The macroecological perspective deliberately sacrifices a great deal of detail in order to see the big picture" (2). Consequently, body size allometry is a great tool for making comparisons or predicting over many orders of magnitude change in body sizes. This requirement does not necessarily rule out metabolic rate predictions microbial communities. Cell volume (V) varies as the radius (r) cubed ($V \propto r^3$), so small changes in size can have a large effect on biomass. The size rage of natural bacterial assemblages is roughly between 0.2 μm to 2 μm, with mass values typically ranging from 10^{-14} to 10^{-11} grams (3).

Metabolic rate refers to the rate by which chemical energy is converted into biological energy and used for either maintenance of existing structure or production of new biomass. Metabolic rate is energy consumption per unit time and is typically measured in Watts or joules of chemical energy degraded to heat every second. For comparison, 4.184 Joules is equal to one Calorie (1). Therefore, whole organism metabolic rate is the amount of energy per unit time that an individual organism requires. It is important to make the distinction between whole organism metabolic

rate (W) and mass specific metabolic rate. Mass specific metabolic rate or the rate of energy expenditure per unit mass is another way to make comparisons among organisms and is typically given in Watts per gram. For metazoans, like fish and mammals, basal metabolic rate scales as $M^{3/4}$, where M is wet mass in grams and mass specific metabolic rate scales as $M^{-1/4}$ (2). This is because $M^{3/4}$ divided by M^{1} equals $M^{-1/4}$. This means that large organisms require more resources than small organisms overall, but flux them through at slower rates. For Bacteria and Archaea, basal metabolic rate scales as $M^{1.7}$, so mass specific metabolic rate scales as $M^{0.7}$ (4).

The Metabolic Theory of Ecology (MTE) predicts the metabolic rate of individual organisms based on the observation that most variation in an individual's metabolic rate can be explained by body size *and* temperature (2, 5). Therefore, the general form of the equation describing whole organism metabolic rate is the same as in Equation 1, but also includes a term to account for the effects of temperature on metabolic rate (I) (Equation 4).

$$I = i_0 M^{\alpha} e^{-E/kT} \qquad \text{Equation 4}$$

Here i_0 is the mass-independent normalization constant, M is the wet weight of the organism in grams, and α is the scaling exponent. The effects of temperature on metabolic rate are accounted for by the term $e^{-E/kT}$ (2,5-6) where E is the average kinetic energy of activation, k is Boltzmann's constant (8.62 x 10^{-5} eV K^{-1}), and T is the temperature (in Kelvin). For endotherms, T would be the average body

temperature; for exotherms this would be the ambient temperature. Boltzmann's constant describes the proportion of molecules with sufficient kinetic energy to exceed the activation energy. According to the Boltzmann distribution, as the temperature is raised the rate of reaction speeds up exponentially. The negative sign in front of E means that as the ratio gets bigger, metabolic rate (I) gets smaller. Therefore, high temperature and low activation energy speed up the rate of reaction. For example, the activation energy of respiration, which is driven by ATP synthesis and is similar for plants and animals, is of greater magnitude than that of oxygenic photosynthesis, controlled by Rubisco carboxylation (6-7). Consequently, an autotrophic microbe would require more energy per gram than a heterotrophic microbe of the same mass. At lower temperatures, autotrophs have an edge over heterotrophs; which may be a factor contributing to seasonal algal blooms in polar regions. Body size and temperature account for most of the variation in individual metabolic rate; however, experimental/measurement error, phylogenetic/environmental constraints, the influence of stoichiometry, and acclimation or adaptation to different conditions can also contribute to the observed variation in metabolic rate (1-2).

The Role of Microbes in the Coral Reef Food Web. In the ocean, the process by which heterotrophic bacterioplankton recover and repackage energy and materials in the form of dissolved organic matter (DOM) into particulate organic matter (POM) is called the Microbial Loop (8). This POM can ultimately be reincorporated into bacterioplankton as DOM via predation-driven remineralization processes; i.e.

"sloppy" predation by heterotrophic nanoflagellates or bacteriophage-mediated DOM release. In the euphotic zone of the open ocean, i.e. oligotrophic waters, where nutrient supply is thought to limit phytoplankton biomass, microbial abundance may be close to a lower threshold (~ 10^5 cells ml^{-1}) (9). Predation by bacterivores and bacteriophage may be less efficient near this lower bound, and the mobilization of nutrients via the microbial loop may be reduced. In oceanic waters, POM in the form of microbial biomass is a substantial fraction of the total POC (> 40%) and it can also be linked back into the larger planktonic food web by the microbial grazers (9). However, due to the large number of inefficient trophic transfers involved, less than 1% of this microbial POM pool is thought to actually make it into fish; most of the carbon that goes into building fish biomass comes from zooplankton and other fish (Azam, pers. comm).

In terms of energy, turnover time is defined as the time required to metabolize an amount of energy equal to the energetic content of the tissues (the amount stored in biomass) (1). In the open ocean, the microbial community typically releases an amount of energy equal to 100% of its body's energy in roughly 2-6 days (10). Relative to macroorganisms, these rates of energy and materials flux are high (11). Yet most studies which have assessed the effects of human activity on coral reef systems emphasize the importance of fish biomass information (12-13). This is not surprising considering global fish stocks have collapsed from roughly 30 million to 3.0 million tonnes per hectare in last 20 years and many of the most threatened marine ecosystem-

types including mangroves, coral reefs, rocky-reefs, and surface waters typically experience multiple types of fishing (14-15). In oceanic and reef systems, even a small increase in microbial biomass can result in substantial changes in whole system rates of energy and materials flux via the microbial loop. By comparison, relatively large reductions in fish biomass, affect the system bioenergetics to a lesser degree. Therefore, in order to understand the mechanism(s) that underlie reef system degradation, we need to understand the effects of rising human impact on the bioenergetics of both organismal components (fish and microbes).

References

1. Peters, RH (1986) The ecological implications of body size. Cambridge University Press, New York, USA.

2. Brown, JH, Gillooly, JF, Allen, AP, Savage, VM and West, GB (2004) Toward a metabolic theory of ecology. Ecol 85: 1771–1789.

3. Malfatti, F, Samo, TJ and Azam, F (2010) High-resolution imaging of pelagic bacteria by Atomic Force Microscopy and implications for carbon cycling. ISME J 4: 427–439.

4. DeLong, JP, Okie, JG, Moses, ME, Sibly, RM and Brown, JH (2010) Shifts in metabolic scaling, production, and efficiency across major evolutionary transitions of life. PNAS 107: 12941.

5. Gillooly, JF, Brown, JH, West, GB, Savage, VM and Charnov, EL (2001) Effects of size and temperature on metabolic rate. Science 293: 2248.

6. Atkins PW (2007) Four laws that drive the universe. Oxford University Press, New York, USA.

7. Allen, A, Gillooly, J and Brown, J (2005) Linking the global carbon cycle to individual metabolism. Funct Ecol 19: 202–213.

8. Azam, F, et al. (1983) The ecological role of water column microbes in the sea. Mar Ecol Prog Ser 10: 257–263.

9. Cho, BC and Azam, F (1990) Biogeochemical significance of bacterial biomass in the ocean's euphotic zone. Mar Ecol Prog Ser. 63: 253–259.

10. Behrenfeld, MJ and Falkowski, PG (1997) A consumer's guide to phytoplankton primary productivity models. Limnol Oceanogr 42:7 1479–1491.

11. McDole, T, et al. (2012) Assessing coral reefs on a Pacific-wide scale using the microbialization score. PLoS ONE 7:9 e43233.

12. Travers, M, Watermeyer, K, Shannon, LJ and Shin, YJ (2010) Changes in food web structure under scenarios of overfishing in the southern Benguela: Comparison of the Ecosim and OSMOSE modelling approaches. J Mar Syst 79:1 101–111.

13. Daskalov, GM, Grishin, AN, Rodionov, S and Mihneva, V (2007) Trophic cascades triggered by overfishing reveal possible mechanisms of ecosystem regime shifts. PNAS 104:25 10518–10523.

14. Halpern, BS, Selkoe, KA, Micheli, F and Kappel, CV (2007) Evaluating and ranking the vulnerability of global marine ecosystems to anthropogenic threats. Cons Biol 21:5 1301–1315.

15. Halpern, BS, et al. (2008) A global map of human impact on marine ecosystems. Science 319: 948–952.

CHAPTER 2

Assessing Coral Reefs on a Pacific-wide Scale Using the Microbialization Score

Abstract

The majority of the world's coral reefs are in various stages of decline. While a suite of disturbances (overfishing, eutrophication, and global climate change) have been identified, the mechanism(s) of reef system decline remain elusive. Increased microbial and viral loading with higher percentages of opportunistic and specific microbial pathogens have been identified as potentially unifying features of coral reefs in decline. Due to their relative size and high per cell activity, a small change in microbial biomass may signal a large reallocation of available energy in an ecosystem; that is the *microbialization* of the coral reef. Our hypothesis was that human activities alter the energy budget of the reef system, specifically by altering the allocation of metabolic energy between microbes and macrobes. To determine if this is occurring on a regional scale, we calculated the basal metabolic rates for the fish and microbial communities at 99 sites on twenty-nine coral islands throughout the Pacific Ocean using previously established scaling relationships. From these metabolic rate predictions, we derived a new metric for assessing and comparing reef health called the microbialization score. The microbialization score represents the percentage of the combined fish and microbial predicted metabolic rate that is microbial. Our results demonstrate a strong positive correlation between reef microbialization scores and human impact. In contrast, microbialization scores did not significantly correlate with

ocean net primary production, local chl*a* concentrations, or the combined metabolic rate of the fish and microbial communities. These findings support the hypothesis that human activities are shifting energy to the microbes, at the expense of the macrobes. Regardless of oceanographic context, the microbialization score is a powerful metric for assessing the level of human impact a reef system is experiencing.

Introduction

The relationship between increasing human activity and decreasing fish biomass is well-established in coral reef systems (1-3). Although herbivore reduction due to overfishing probably facilitates coral to algal transitions, the mechanistic link between overfishing and coral mortality is not clear (4). Much uncertainty about the mechanisms of reef decline linked to eutrophication and climate change also still exists (5-6). In addition to increasing algal cover relative to hard coral cover, other effects of anthropogenically-driven disturbances include disease outbreaks, fewer links in trophic webs, and loss of physical structure and habitat complexity (7-9). Reef-associated microbial communities have been shown to respond to all of the above disturbances (overfishing, nutrient enrichment, thermal stress) by becoming less beneficial and more pathogenic, i.e. the proportion of sequences related to known pathogens typically increases (10-17).

Despite the epidemiological evidence linking the microbial ecology of coral reef systems to human activity, the largest study of coral reef microbial communities included only four coral atolls in the Line Islands, all clustered within one oceanographic region (14). In this island chain a 10-fold increase in microbial and viral abundances in the overlying reef-water correlated with increasing human disturbance and was accompanied by decreased fish biomass (1, 14). Further, a large proportion of the microbial 16S rDNA sequence similarities on the most disturbed

reefs were most closely related to known pathogens (14). These reefs also had the highest incidences of coral disease and the lowest percent coral cover. Other studies have also suggested that the total carbon flow through microbial pathways via detritus is inversely related to coral cover (18-19).

Ecosystems exhibit higher-level properties resulting from lower-level phenomena (20). The energy available to a higher trophic level, for example, is reduced by the amount required to support the individual organisms in the lower level. The Metabolic Theory of Ecology (MTE) predicts the metabolic rate of individual organisms based on the observation that most variation in an individual's metabolic rate can be explained by body size and temperature (21, 22). Whole organism metabolic rate (*I*), defined as the amount of energy per unit time that an individual organism requires, is calculated using Equation 1:

$$I = i_0 M^{\alpha} e^{-E/kT} \qquad \text{(Equation 1)}$$

where i_0 is the mass-independent normalization constant, M is the wet weight of the organism in grams, and α is the scaling exponent. The effects of temperature on metabolic rate are accounted for by $e^{-E/kT}$ (21, 23) where E is the activation energy, k is Boltzmann's constant (8.62×10^{-5} eV K^{-1}), and T is the water temperature at the site at the time of collection (in Kelvin). Distinct scaling exponents have been derived for different physiological states and evolutionary groups (21, 24-25).

The process of replacing macroorganisms with microbes has been termed *microbialization* (26). In this study, Equation 1 was used to predict metabolic rates for all individual fish and microbes present in a 10 m^3 volume of reef water. *Microbialization* refers to an increase in the percentage of the combined fish and microbial predicted metabolic rate that is microbial. Island-level microbialization scores were derived for 29 islands (99 sites) within four oceanographic regions of the Pacific Ocean. Our data show a strong significant positive correlation between microbialization scores and the NCEAS cumulative human impact scores at each island. In comparison, microbialization scores did not correlate with the net primary production values. These findings support the hypothesis that human activities rather than variation in oceanographic conditions are causing microbialization of coral reefs and that the microbialization score is a powerful metric for assessing and comparing reef health.

Materials and Methods

Site descriptions: The twenty-nine islands included in this study were surveyed following the National Oceanic and Atmospheric Association (NOAA)'s Rapid Ecological Assessment (REA) protocol as part of the Coral Reef Ecosystem Division (CRED) and Pacific Reef Assessment and Monitoring Program (Pacific RAMP) (27). Multiple coral reef sites (average depth: 10 m) were sampled at each island in four broad regional groups: the Main Hawaiian Islands (MHI), Guam and the Mariana

Islands (MARIANA), the American Samoa region (SAMOA), and the Pacific Remote Island Areas (PRIA) (Fig. 1, Table 1). Microbial samples were collected during the 2008-2010 Pacific RAMP monitoring cruises: MHI (2008), MARIANAS (2009), SAMOA (2010), PRIA (2010). For fish, belt survey data from 2001-2009 was used for all islands. Because the REA survey protocol switched to the Stationary Point Count (SPC) method in 2009, 2010 fish data was not included. Microbial and fish data collection sites at each island are not necessarily co-located. Due to the variability inherent with observational fish data, the standard approach for estimating island means for fish abundance requires a large sample size. To have an adequate sample size, this fish data was pooled from all sites and years. Island-level averages and standard errors for fish and microbial biomass are provided in Table S2 and Fig. S2. Microbial metabolic rates were calculated per site then averaged by island. Island-level averages for fish and microbial predicted metabolic rates were used to calculate one microbialization score for each island.

Collection of microbial data: At each site, 4 replicate 2 l seawater samples were collected ~1 m above the benthos using polycarbonate Niskin bottles. Microscopy grade glutaraldehyde was added to a final concentration of 0.3% v/v. Microbial cells were collected from each sample by filtration using a 0.2 μm Anodisc filter (Whatman) and then stained with 5 μg ml^{-1} DAPI (Molecular Probes, Invitrogen) within 2 hours of collection (28-30). Filters were mounted on microscope slides and stored at -20 °C. For each site, 10 fields of view (5 fields for each of 2 replicate filters,

~200 cells per field) were examined by epifluorescence microscopy (excitation/emission: 358/461 nm) at 600X magnification. Cell counts and dimensions were collected using ImagePro Software (Media Cybernetics) set for a size range of 0.00001 – 10 μm for both length and width. Cell volume (*V*) was calculated by considering all cells to be cylinders with hemispherical caps using Equation 2:

$$V = \pi/4 \times w^2 \left(l - w/3\right) \qquad \text{(Equation 2)}$$

where *l* is length and *w* is width (31). No correction was made for possible cell shrinkage as a result of fixation. Individual microbial cell volumes *V* (μm^3) were converted to mass in wet weight (g) using previously established size-dependent relationships for marine microbial communities (32). Each cell volume *V* was next converted to dry weight using the linear relationship derived from data reported in Simon and Azam (1989) and shown in Equation 3:

$$\log\left(y\right) = 1.72 \log\left(x\right) - 12.63 \qquad \text{(Equation 3)}$$

where *x* is cell dry weight and *y* is cell volume (r^2=0.99). Then cell wet weight (*z*) was calculated using the linear relation shown in Equation 4 (32) (r^2 = 0.99):

$$\log\left(z\right) = 1.63 \log\left(x\right) - 2.0 \qquad \text{(Equation 4)}$$

Collection of fish data: This study includes fish data from all surveys performed at REA sites during the years 2001–2009. The number of REA sites surveyed over this time period is provided for each island in Table S2. Visual surveys provided a census of the reef fish community (33). Surveys were restricted to shallow-to-moderate depths along the forereef between 10-15 m with a majority of surveys completed along the 10m isobaths. At each site, a total of three 25 m long belt transect surveys were conducted by two different divers. For each survey, the diver made two passes: during the first pass, all fish > 20 cm in length were recorded in adjacent 4 m wide belts; during the second pass all fish ≤ 20 cm were recorded in 2 m wide belts. Lengths were recorded to the nearest cm for fish < 5 cm and in 5 cm bins for all others (34). Species-specific mass values for individual fish were calculated from length-weight relationships using FishBase (35-36). The fish data was provided for each family as mean biomass (g m^{-2}) and mean abundance (# individuals m^{-2}), from which the mean mass per individual (g) was calculated. Because surveys were carried out at an average water depth of 10 m and surveyors counted all fish in the water column up to the surface, the mean abundances (individuals per m^2) represented the total number present in a 10 m^3 water column.

Metabolic rate calculations: At each REA site, community-level metabolic rates were calculated by summing the individual metabolic rates (*I*) for all fish or microbes present in a standard volume of water (10 m^3). Individual metabolic rates (*I*) in watts were calculated using Equation 1.

The mass independent normalization constant for fish, i_0, ($\ln(i_0)$ =18.47) was extracted from the plots in Brown et al. (21), while those for basal and active microbial states (4.61×10^{16} and 1.08×10^{21}, respectively) were calculated from previously reported individual prokaryote metabolic rate values (25). The predicted scaling exponents (α) used for microbes were 1.72 (basal) and 1.96 (active) (25), while 0.71 was used for fish (21). The activation energies (*E*) used were 0.61 eV for microbes (25) and 0.69 eV for fish (21).

Quantification of human impact: The level of human impact was assessed from the cumulative global human impact map generated by the National Center for Ecological Analysis and Synthesis (NCEAS; http://www.nceas.ucsb.edu/globalmarine/impacts). Using ArcGIS 9.3, "NoData" pixels corresponding to the land mass of each island were identified and converted into polygon format. A 10 km zone was then calculated for each of these polygons, representing the immediate 10 km of sea surface around the border of each island in the study. Using these zones, statistics were then performed on the NCEAS human impact raster in order to calculate the mean impact score. These scores incorporate data related to: artisanal fishing; demersal destructive fishing; demersal non-destructive, high-bycatch fishing; demersal non-destructive low-bycatch fishing; inorganic pollution; invasive species; nutrient input; ocean acidification; benthic structures (e.g., oil rigs); organic pollution; pelagic high-bycatch fishing; pelagic low-

bycatch fishing; population pressure; commercial activity (e.g., shipping); and anomalies in sea surface temperature and ultraviolet insolation.

Other indicators of reef system health were also considered in this study using benthic survey data collected at the same time as the microbial data. Benthic surveys were performed using the survey methodology described in Vargas-Angel (37-38). A principal components analysis was carried out using R on the following initial variables: coral disease prevalence, prevalence of coral colonies with compromised health (unidentified sub-lethal lesions including algal and cyanophyte interactions, and barnacle and tubeworm infestations), percent crustose corraline algae cover, percent coral cover, and the microbialization score (39, 40). Raw data sets were rescaled to give mean 0 and standard deviation of 1. As a supplement to PCA analysis, *k*-means clustering was also performed on the same data matrix for k = 2-8 (100 iterations); the dissimilarity matrix was calculated using Gower's standardization (41).

Estimation of net primary production: Productivity estimations for net primary productivity (NPP) (mg C m^{-2} day^{-1}) were derived from Moderate Resolution Imaging Spectroradiometer (MODIS) satellite data using the Vertically Generalized Production Model (VGPM; http://www.science.oregonstate.edu/ocean.productivity/standard.product.php). This model, based on an algorithm by Behrenfeld and Falkowski (1997) calculates net primary production from satellite-based measurements of surface chl*a* concentrations,

while also taking into account sea surface temperature, daily photosynthetically active radiation, and a temperature-dependent photosynthetic efficiency factor (42). Because these satellite data sets are less accurate for near-shore measurements, the satellite-based NPP values used here were estimated from the data for a 50 km radius ring surrounding each island, with the first 10 km around each island removed. The nearshore chl*a* concentrations ($\mu g\ l^{-1}$) used in this study were obtained using fluorometric analysis (43). The chl*a* samples were collected in conjunction with the microbial samples at each site.

Results and Discussion

Predicted metabolic rates for the fish and microbes: Field surveys carried out at 99 coral reef sites at 29 Pacific islands (Fig. 1) were used to calculate the biomass (g per 10 m^3) and basal metabolic rate (W per 10 m^3) for both the water column-associated microbial and fish communities (Table 1). The high and low values for microbial biomass occurred on the islands of Oahu (1.53 g per 10 m^3) and Wake Atoll (0.12 g per 10 m^3), respectively. This difference in microbial biomass equates to a 76-fold increase in the rate of energy flux (W per 10 m^3 or J sec^{-1} 10 m^{-3}) on Oahu (0.076 W per 10 m^3) relative to Wake Atoll (0.001 W per 10 m^3). The highest fish biomass was found on Kingman (514.84 g per 10 m^3) and the lowest on Guam (17.98 g per 10 m^3). The metabolic requirements predicted for the fish communities on Kingman and Guam were 0.015 and 0.002 W per 10 m^3, respectively. This difference equates to a 7.5-fold reduction in the metabolic requirements of the fish community. The largest

differences in the predicted metabolic rates between each island represent a 100-fold change for the microbes, as compared to a 14-fold change for the fish (Table 1).

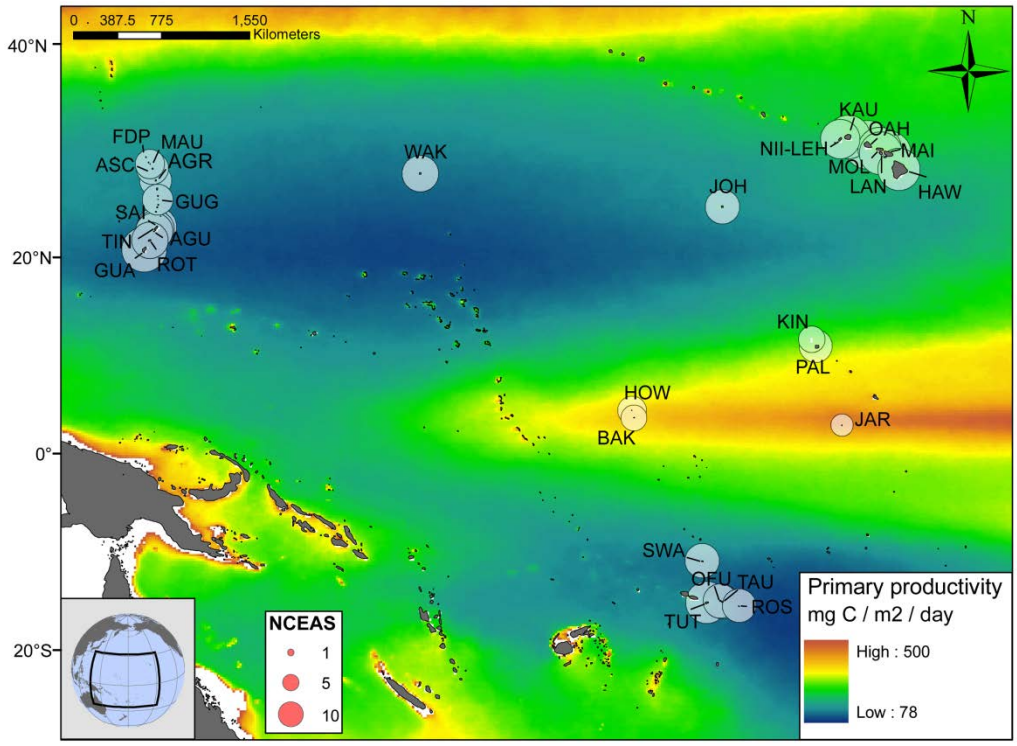

Figure 2.1 Location of the 29 islands surveyed. Color scale indicates oceanic net primary production derived from satellite data using the Vertically Generalized Production Model (VGPM). Circles indicate the relative NCEAS cumulative human impact score for each island. For island abbreviations see Table 1.

Table 2.1 Survey data and calculated values for 29 islands in the Pacific, grouped by region. Predicted metabolic rates are basal rates. NPP = net primary production. Colors identify each island group in the figures.

REGION		**MICROBIAL COMMUNITY**			**FISH COMMUNITY**		**OTHER**		
Code	Island	Abundance x 10^5	Total Biomass	Predicted Metabolic Rate	Total Biomass	Predicted Metabolic Rate	NPP	Chla	NCEAS Score
		cells ml^{-1}	g 10 m^{-3}	W 10 m^{-3}	g 10 m^{-3}	W 10 m^{-3}	mg C m^{-2} yr^{-1}	µg l^{-1}	
GUAM & MARIANA ISLANDS (orange)									
AGR	Agrihan	2.6	0.22	0.005	84.54	0.007	155	0.11	7.7
AGU	Aguijan	2.3	0.16	0.006	41.5	0.005	125	0.34	9.9
ASC	Asuncion	2.7	0.15	0.002	182.54	0.011	159	0.11	7.6
FDP	Farallon de Pajaros	2.7	0.2	0.003	103.18	0.007	165	0.06	6.8
GUA	Guam	2.8	0.27	0.012	17.98	0.002	126	0.17	13.7
GUG	Guguan	3.5	0.27	0.002	145.03	0.012	153	0.1	7.1
MAU	Maug	3	0.24	0.003	70.95	0.005	159	0.22	6.7
ROT	Rota	2.3	0.17	0.003	36.9	0.004	125	0.07	9.4
SAI	Saipan	2.1	0.21	0.017	23.31	0.003	143	0.1	11.2
TIN	Tinian	1.8	0.17	0.004	31.19	0.003	143	0.05	10.3
MAIN HAWAIIAN ISLANDS (MHI, blue)									
HAW	Hawaii	4.7	0.81	0.012	51.24	0.004	248	0.12	12.2
KAU	Kauai	2.8	0.69	0.024	33.39	0.002	262	0.34	13
LAN	Lanai	3.3	0.4	0.007	33.44	0.002	264	0.15	12.7
MAI	Maui	3	0.56	0.019	40.16	0.003	258	0.21	14.2
MOL	Molokai	2.1	0.32	0.006	24.8	0.002	270	0.1	12.8
NII/LEH	Niihau & Lehua	4.1	1.29	0.05	54.49	0.003	234	0.22	10.7
OAH	Oahu	3.7	1.53	0.076	23.99	0.002	270	0.19	15.6
PACIFIC REMOTE ISLANDS & ATOLLS (PRIA, pink)									
BAK	Baker	3.8	0.33	0.004	228.18	0.011	380	0.1	5.3
HOW	Howland	4.5	0.49	0.014	195.37	0.022	380	0.06	6.3
JAR	Jarvis	5.8	0.46	0.005	408.75	0.026	445	0.08	4
JOH	Johnston	3.5	0.72	0.024	91.6	0.005	196	0.09	8.5
KIN	Kingman	1.7	0.18	0.002	514.84	0.015	282	0.11	5.5
PAL	Palmyra	3.7	0.22	0.002	229.08	0.01	307	0.16	8
WAK	Wake	2.2	0.12	0.001	161.4	0.008	147	0.06	9.5
SAMOA REGION (green)									
OFU/OLO	Ofu & Olosega	2.9	0.19	0.003	57.83	0.004	139	0.07	8.4
ROS	Rose	3.2	0.14	0.002	82.98	0.007	130	0.04	8.2
SWA	Swains	3.1	0.26	0.004	85.17	0.005	148	0.04	8.6
TAU	Tau	3.3	0.23	0.004	44.77	0.004	139	0.06	8.6
TUT	Tutuila	3.5	0.25	0.006	33.11	0.003	151	0.15	12.4

Microbialization scores versus the NCEAS human impact score: Based on the predicted metabolic rates for fish and microbes (Table 1), we are proposing a separate metric called the *microbialization score*, which represents the microbial share of the total predicted metabolic rate. The microbialization score is the percentage of the combined fish and microbial predicted metabolic rate that is microbial:

$$\left(\mathrm{W}\ 10\ \mathrm{m}^3{}_{microbes}\right)\Big/\left(\mathrm{W}\ 10\ \mathrm{m}^3{}_{microbes}+\mathrm{W}\ 10\ \mathrm{m}^3{}_{fish}\right)\times 100 \qquad \text{(Equation 5)}$$

Although both increased microbial biomass and decreased fish biomass affect microbialization scores, microbial biomass has a proportionately greater impact on the combined predicted metabolic rate. For example, on Oahu, the fish are responsible for only 3% of the combined predicted metabolic rate, but account for 94% of the total biomass. Even on Kingman where we observed the highest fish biomass and microbial biomass represented less than 0.03% of the total biomass, the microbes still account for 13% of the combined predicted metabolic rate.

Recently, the NCEAS human impact score has been proposed as a cumulative metric of different anthropogenic stressors ranging from overfishing to predicted climate change events (44). As shown in Fig. 2, the microbialization score is positively correlated with the NCEAS score (linear regression, $r^2 = 0.68$; Fig. 2). The microbialization scores ranged from 8% at remote and relatively pristine Wake Island

to 75–98% in the heavily-impacted main Hawaiian Islands (MHI). Oahu, with the highest microbialization score (98%) also had the highest NCEAS score (15.59).

Johnston Atoll in the PRIA group appears to be an exception to the overall trend in that it has a high microbialization score (82%) but a relatively low NCEAS score (8.48). In actuality, Johnston is heavily impacted by factors not reflected in the NCEAS scores including the addition of two artificial islands with paved runways formed by coral dredging, usage for both above-ground and underground nuclear tests in the 1950s and 1960s, and service as a chemical weapons depot until 2000. The microbialization score appears to be a better indicator of these stressors than the NCEAS index of human impact.

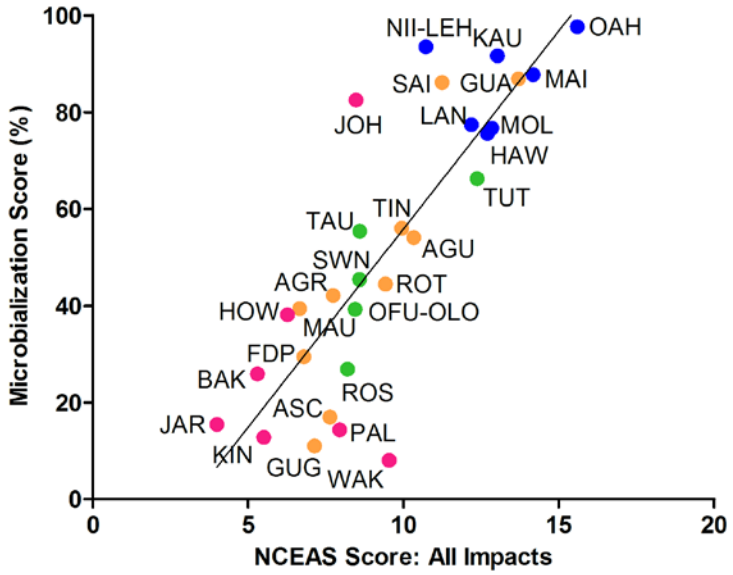

Figure 2.2 Linear regression analysis of microbialization scores versus NCEAS cumulative human impact values ($y = 8.19 x – 26.10$; $r^2 = 0.68$). The microbialization score is the percentage of the combined fish and microbial predicted metabolic rate that is microbial. Color denotes oceanographic region: Guam and the Mariana Islands (orange circles), the Main Hawaiian Islands (blue circles), Pacific Remote Islands and Atolls (pink circles), and the Samoa region (green circles). For island abbreviations see Table 1.

A principal components analysis was carried out with the goal of visualizing how the microbialization score related to other indicators of reef health, including coral disease prevalence, prevalence of coral colonies with other signs of compromised health, percent crustose corraline algae cover, and percent coral cover (Fig. S1). The first two components accounted for 66% of the variation. The first component (PC1) accounted for 46% of the variation and was driven in the positive direction (relative to 0) by coral disease incidence, other visible signs of compromised coral health, and microbialization score (Fig. S1). A complete table of PCA loadings is

provided in Table S3. By comparison, variables which typically correlate positively with reef system health (% crustose coralline algal cover and % coral cover) were represented as vectors moving in the negative direction (relative to 0). The separation by vector sign along PC1 supports the hypothesis that the microbialization score is a useful measure of reef system decline. Because the PCA analysis indicated that there was separation in the data, we used k-means clustering as a supplementary analysis to determine how many groups there were. K-means is a classical variance-based clustering method that defines *n* data points in *d* dimensions, into *k* clusters, so that the within clusters sun-of-squares is minimized (41). The within group sum of squares plotted against the number of clusters (*k*) indicated $k = 3$ to be the optimal number (for $k = 2$-8). The 11 islands contained in cluster two (within-cluster sum of squares = 1.47) were negative for PC1 (Fig. S1), while the 16 islands contained in cluster 3 were all positive on PC1 (within-cluster sum of squares = 2.06). The two islands in the first *k*-means cluster were Lanai (LAN) and Guam (GUA) (within cluster sum-of-squares = 0.32).

Microbialization scores versus combined metabolic rate: The metabolic rates predicted for the combined microbial and fish communities at the 29 islands ranged by approximately one order of magnitude, from a low of 0.007 W per 10 m^3 on Rota Island (MARIANA) to a high of 0.077 W per 10 m^3 on Oahu (MHI) (Fig. 3, x-axis). The combined predicted metabolic rate was not correlated with the microbialization score, which also varied widely among the islands, ranging from a low of 8% at Wake

to a high of 97% at Oahu (Fig. 3, y-axis). At the low end of this scale, increased microbalization scores were explained by reduced metabolic contribution from the fish. However, higher microbialization scores were associated with a sharp rise in combined predicted metabolic rate driven primarily by increasing microbial metabolic rates. This break-point may reflect the release of the microbes from some resource limitation.

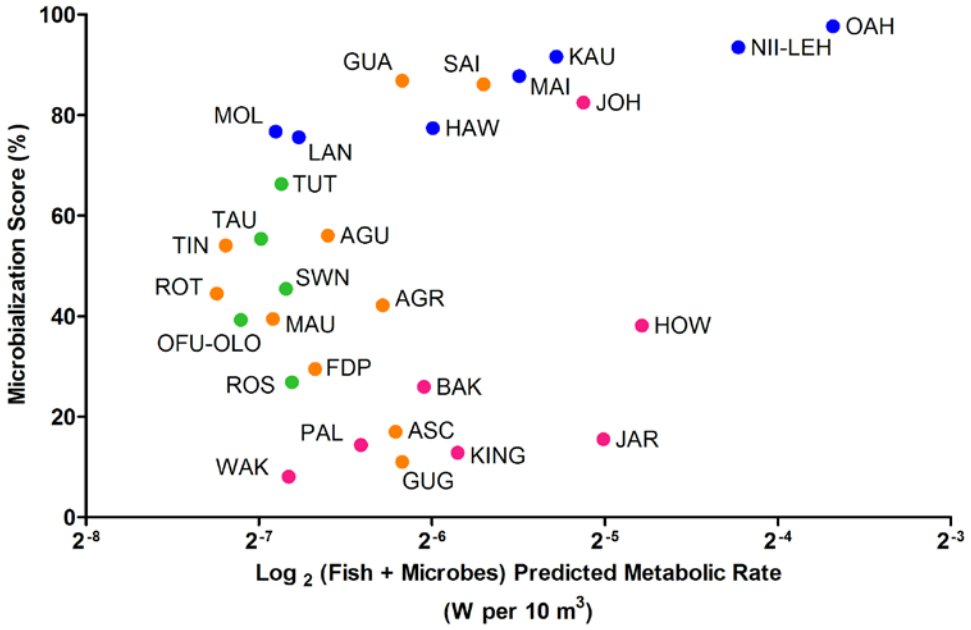

Figure 2.3. Microbialization scores plotted against the combined fish + microbes predicted metabolic rates for each of the 29 islands surveyed. Colors are as in Fig. 2. For island abbreviations see Table 1.

Predicted metabolic rates of fish and microbes versus primary production: Net primary production (NPP) might be expected to be a significant factor driving variation in community metabolic rates. Previous small-scale inter-island studies that correlated differences in microbial communities with varying local human impacts could not conclusively rule out inter-island variations in oceanographic conditions as a possible driving factor (14). To address this issue, we surveyed net primary production (NPP) at islands in four oceanographic regions throughout the Pacific Basin (Table 1).

Estimated net primary production (NPP; mg C m^{-2} day^{-1}) derived from satellite data is shown in Fig. 1. NPP ranged from 125 mg C m^{-2} day^{-1} at Aguijan to 445 mg C m^{-2} day^{-1} at Jarvis (Table 1). This predicted NPP was not a strong predictor of the combined fish + microbial metabolic rate at the island-level (non-linear regression, R^2 = 0.21; Fig. 4A). Likewise, when the predicted NPP values were compared against the metabolic rates of the fish and microbial communities separately, R^2 values were 0.20 for fish and 0.054 for microbes (Table 1). Large differences in NPP were observed between the geographic regions surveyed, but relatively little variation within each one (Fig. 4A, C). Since the satellite data used for the above predictions omitted a 10 km ring around each island, nearshore chl*a* concentrations were also measured as an alternative proxy for NPP. These samples were collected with the microbial samples at each site. The nearshore chl*a* concentrations (μg l^{-1}) explained even less of the inter-island variation in combined predicted metabolic rate (non-linear regression, R^2 =

0.08; Fig. 4B). For the individual communities, R^2 values were 0.13 and 0.15 for fish and microbes, respectively (Table 1).

Microbialization scores and primary production: The island microbialization scores did not correlate with predicted oceanic NPP values (Fig. 4C, $R^2 = 0.004$) or nearshore chl*a* concentrations (Fig. 4D; $R^2 = 0.22$). However, higher nearshore chl*a* concentrations associated with microbialization scores above a certain threshold (~70%) are suggestive of eutrophication processes linked to human impact (Fig. 4D) (45). These analyses demonstrate that estimated reef primary production is not a significant driver of variation in either community metabolic rates or microbialization scores.

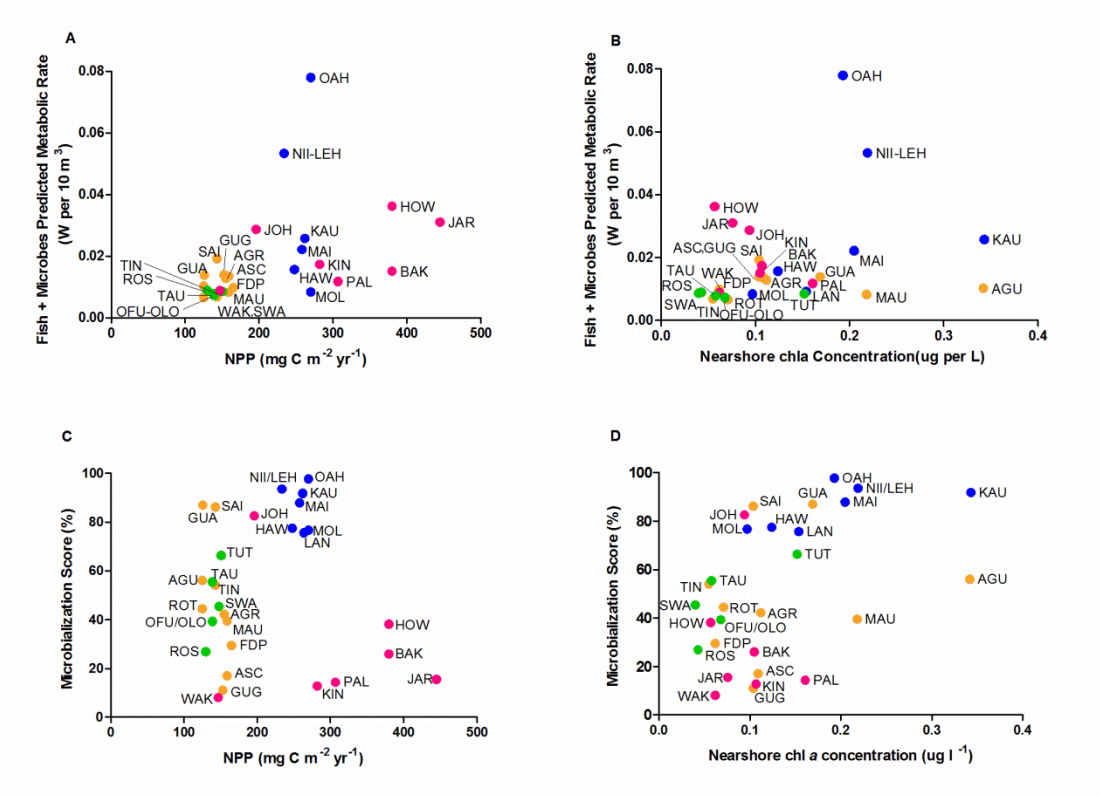

Figure 2.4. Measures of energy use versus metrics of primary production. (a) Non-linear regression analysis of the combined fish + microbes predicted metabolic rate versus net primary production (NPP) for the 29 surveyed islands. NPP was derived from satellite data using the Vertically Generalized Production Model (VGPM). ($y = 0.00008x + 0.0012$; $R^2 = 0.21$) **(b)** Non-linear regression analysis of the combined fish + microbes predicted metabolic rate versus nearshore chl*a* concentrations at the 29 surveyed islands ($y = 0.54x + 0.01$; $R^2 = 0.08$) **(c)** Microbialization scores versus NPP derived from satellite data using the VGPM for the 29 surveyed islands. **(d)** Microbialization scores versus nearshore chl*a* concentrations at the 29 surveyed islands ($y = 171.5x + 29.7$; $R^2 = 0.22$). Colors are as in Fig. 2. For island abbreviations see Table 1.

To further examine whether or not accounting for oceanographic context would improve our ability to predict reef microbialization, multiple linear regression analysis was performed. In addition to the NCEAS score, satellite-based estimates of net primary production (NPP) and nearshore (chl*a*) were included as variables. This

resulted in 4 models of interest: microbialization score = $\beta_0 + \beta_1(\text{NCEAS})$, $y = \beta_0 + \beta_1(\text{NCEAS}) + \beta_2(\text{chl}a)$, $y = \beta_0 + \beta_1(\text{NCEAS}) + \beta_2(\text{NPP})$, $y = \beta_0 + \beta_1(\text{NCEAS}) + \beta_2(\text{chl}a) + \beta_3(\text{NPP})$. Given that the NCEAS score was in the model, the p-values for chl*a* and NPP were not significant by the t-test in the second and third models (p-value > 0.1). The only variable that was significant was the NCEAS score, having a highly significant p-value in all of the models (p-value < 0.0001). The model which included both chl*a* and NPP as variables ($y = \beta_0 + \beta_1(\text{NCEAS}) + \beta_2(\text{chl}a) + \beta_3(\text{NPP})$) gave a multiple R^2 value of 0.706, which was not a significant improvement over the simplest model ($y = \beta_0 + \beta_1(\text{NCEAS})$) which explained 68.4 % of the variability of the microbialization score.

Next, Akaike's Information Criterion (AIC) was used for model selection between the 4 different statistical models. AIC is the most widely known and used model selection criterion which consists of a "goodness-of-fit" term and a "penalty" term for increased number of model parameters (46). The model with the lowest AIC value is selected as the best model. The model having the smallest AIC was the model which did not include additional variables ($y = \beta_0 + \beta_1(\text{NCEAS})$). Although the exact mechanism(s) underlying the *process* of microbialization remain unclear, these analyses support the hypothesis that human activities alter the energy budget of the reef system, specifically by altering the allocation of metabolic energy between microbes and macrobes.

The finding that microbialization scores did not significantly correlate with ocean net primary production, local chl*a* concentrations, or the combined metabolic rate of the fish and microbial communities suggests that the microbialization score may be a powerful metric for comparing and assessing reef degradation, particularly at large spatial scales. Other measures of reef degradation which are more heavily influenced by oceanographic context (i.e. percent coral cover, percent algal cover) may be more easily confounded by non-human factors and are subsequently harder to interpret across large spatial scales.

Other considerations: In this study, surveys of microbial and fish sizes were used to predict whole organism metabolic rates. Ideally, the energetic requirements per unit time for fish and microbial communities would be measured empirically. However, this is not practical over this large region. To evaluate whether or not the MTE-based approach is a reasonable alternative to quantifying energy flux, the mean predicted metabolic rates for microbial communities were compared against experimental values reported from other studies (Table S1). The means for both the predicted basal metabolic rates used in our analyses and the corresponding predicted active metabolic rates fall within the same range as the empirically-based measurements. Similarly, differences in temperature at the time of sampling explained a small proportion of the variation in metabolic rate between islands. Water temperature at the time of sampling ranged from 25 – 30°C. For the microbial community-level metabolic rates, the standard deviation in the 29 island data set was

0.16 at the actual temperatures and 0.01 when all locations were corrected to the same temperature (20°C); for the fish community-level metabolic rates, the standard deviations were 0.006 and 0.003, respectively. Temperature correction increased the r^2 value for the regression analysis of community-level metabolic rate as a function of biomass by only 0.01% and 0.05% for fish and microbes, respectively. Therefore, inter-island variation in temperature does not account for our observed trends.

Conclusions

Overfishing, eutrophication, and global climate change are important drivers of the global loss of coral reefs. However, the precise mechanism(s) by which these perturbations lead to coral decline have remained elusive. We and others have previously argued that human activities are favoring the coral reef-associated microbes at the expense of the macrobes, a process called *microbialization*. The data presented here supports this hypothesis over a wide swath of Pacific coral reefs and suggests that microbialization is a general process of reef decline. Although the exact mechanism(s) driving the process of microbialization remain unclear, the microbialization score provides a way to diagnose the degree of microbialization that has occurred on reefs. Fish were the primary movers of energy in the most pristine locations (i.e. fish were responsible for 97 and 87% of the total predicted metabolic rate on Wake (PRIA) and Kingman (PRIA), respectively) but made up only 3% of the total predicted metabolic rate on Oahu (MHI). Microbialization scores reflect both increased microbial biomass and decreased fish biomass; however microbial biomass has a proportionately greater

impact on metabolic rate. This means that even a minor increase in the microbial load results in a substantial shift in community energy use**;** up to a 100-fold increase in the metabolic requirements of the microbes in the most heavily impacted reef systems**.** This study has significant implications for the protection of coral reefs. The degree of microbialization a reef is experiencing may be important for predicting its response to perturbation. On Pacific coral reefs, *microbialization* may be set in motion by an increase in the percent cover of turf algae resulting from the loss of herbivorous fish. Turf algae release large amounts of dissolved organic carbon (DOC) into the water column, a source of energy almost exclusively available to the microbes (47). Consequently, the process of microbialization is likely to have stabilization effects in the system once a catastrophic regime shift to an algal-dominated state has occurred.

References

1. Sandin SA, Smith JE, DeMartini EE, Dinsdale EA, Donner SD, et al. (2008) Baselines and degradation of coral reefs in the Northern Line Islands. PLoS ONE 3: e1548.

2. Knowlton N, Jackson JBC (2008) Shifting baselines, local impacts, and global change on coral reefs. PLoS Biol 6: e54.

3. DeMartini EE, Friedlander AM, Sandin SA, Sala E (2008) Differences in fish-assemblage structure between fished and unfished atolls in the northern Line Islands, central Pacific. Mar Ecol Prog Ser 365: 199–215.

4. Maliao RJ, Turingan RG, Lin J (2008) Phase-shift in coral reef communities in the Florida Keys National Marine Sanctuary (FKNMS), USA. Mar Biol 154: 841-853.

5. Bourne DG, Garren M, Work TM, Rosenberg E, Smith GW, et al. (2009) Microbial disease and the coral holobiont. Trends Microbiol 17: 554-562.

6. Sokolow S (2009) Effects of a changing climate on the dynamics of coral infectious disease: a review of the evidence. Dis Aquat Org 87: 5-18.

7. Essington TE, Beaudreau AH, Wiedenmann J (2006) Fishing through marine food webs. Proc Natl Acad Sci USA 103: 3171-3175.

8. Greenstein BJ, Curran HA, Pandolfi JM (1998) Shifting ecological baselines and the demise of *Acropora cervicornis* in the western North Atlantic and Caribbean Province: a Pleistocene perspective. Coral Reefs 17: 249-261.

9. McCormick M (1994) Comparison of field methods for measuring surface topography and their association with a tropical reef fish community. Mar Ecol Prog Ser 112: 87–96.

10. Thurber RLV, Barott KL, Hall D, Liu H, Rodriguez-Mueller B, et. al. (2008) Metagenomic analysis indicates that stressors induce production of herpes-like viruses in the coral *Porites compressa.* Proc Natl Acad Sci USA 105: 18413-18418.

11. Bruno JF, Petes LE, Harvell DC, Hettinger A (2003) Nutrient enrichment can increase the severity of coral diseases. Ecol Lett 6: 1056-1061.

12. Bruno JF, Selig ER, Casey KS, Page CA, Willis BL, et al. (2007) Thermal stress and coral cover as drivers of coral disease outbreaks. PLoS Biol 5:e124.

13. Kuntz NF, Kline DI, Sandin SA, Rohwer F (2005) Pathologies and mortality rates caused by organic carbon and nutrient stressors in three Caribbean coral species. Mar Ecol Prog Ser 294: 173–180.

14. Dinsdale E, Pantos O, Smriga S, Edwards RA, Angly F, et al. (2008) Microbial ecology of four coral atolls in the Northern Line Islands. PLoS ONE 3: e1584.

15. Mao-Jones J, Ritchie KB, Jones LE, Ellner SP (2010) How microbial community composition regulates coral disease development. PLoS Biol 8: e1000345.

16. Mouchka ME, Hewson I, Harvell CD (2010) Coral-associated bacterial assemblages: current knowledge and the potential for climate-driven impacts. Int Comp Biol 50: 662 -674.

17. Kelly, LW, et al. (2012) Black reefs: iron-induced phase shifts on coral reefs. ISME J 6: 638–649

18. Johnson C, Klumpp D, Field J, Bradbury R (1995) Carbon flux on coral reefs: effects of large shifts in community structure. Mar Ecol Prog Ser 126: 123–143.

19. Arias-Gonzalez J, Delesalle B, Salvat B, Galzin R (1997) Trophic functioning of the Tiahura reef sector, Moorea Island, French Polynesia. Coral Reefs 16: 231–246.

20. Ernest SKM, Enquist BJ, Brown JH, Charnov EL, Gillooly JF, et al. (2003) Thermodynamic and metabolic effects on the scaling of production and population energy use. Ecol Lett 6: 990–995.

21. Brown JH, Gillooly JF, Allen AP, Savage VM, West GB (2004) Toward a metabolic theory of ecology. Ecology 85: 1771–1789.

22. Gillooly JF, Brown JH, West GB, Savage VM, Charnov EL (2001) Effects of size and temperature on metabolic rate. Science 293: 2248.

23. Atkins PW (2007) Four laws that drive the universe. New York: Oxford University Press.

24. Peters RH (1986) The ecological implications of body size. New York: Cambridge University Press.

25. DeLong JP, Okie JG, Moses ME, Sibly RM, Brown JH (2010) Shifts in metabolic scaling, production, and efficiency across major evolutionary

transitions of life. Proc Natl Acad Sci USA 107: 12941.

26. Jackson JBC, Kirby MX, Berger WH, Bjorndal KA, Botsford LW, et al. (2001) Historical overfishing and the recent collapse of coastal ecosystems. Science 293: 629.

27. Waddell, JE and AM Clark (eds) 2008. The state of coral reef ecosystems of the United States and Pacific Freely Associated States: 2008. NOAA Technical Memorandum NOS NCCOS 73. NOAA/NCCOS Center for Coastal Monitoring and Assessment's Biogeography Team. Silver Spring, MD.

28. Hobbie JE, Daley RJ, Jasper S (1977) Use of nuclepore filters for counting bacteria by fluorescence microscopy. Appl Environ Microbiol 33: 1225.

29. Porter KG, Feig YS (1980) The use of DAPI for identifying and counting aquatic microflora. Limnol Oceanogr 25: 943–948.

30. Noble RT, Fuhrman JA (1998) Use of SYBR Green I for rapid epifluorescence counts of marine viruses and bacteria. Aquat Microb Ecol 14: 113–118.

31. Bjornsen PK (1986) Automatic determination of bacterioplankton biomass by image analysis. Appl Environ Microbiol 51: 1199.

32. Simon M, Azam F (1989) Protein content and protein synthesis rates of planktonic marine bacteria. Mar Ecol Prog Ser 51: 201–213.

33. Brock RE (1982) A critique of the visual census method for assessing coral reef fish populations. Bull Mar Sci 32: 269–276.

34. Williams ID, Walsh WJ, Schroeder RE, Friedlander AM, Richards BL, et al. (2008) Assessing the importance of fishing impacts on Hawaiian coral reef fish assemblages along regional-scale human population gradients. Environ Conserv 35: 261–272.

35. Froese R, Pauly D (1994) Fishbase as a tool for comparing the life history patterns of flatfish. Neth J Sea Res 32: 235–239.

36. Kulbicki M, Guillemot N, Amand M (2005) A general approach to length-weight relationships for New Caledonian lagoon fishes. Cybium 29: 235–252.

37. Vargas-Angel B (2009) Coral health and disease assessment in the US Pacific Remote Island Areas. Bull Mar Sci 84: 211–227.

38. Vargas-Angel B, Looney EE, Vetter OJ, Coccagna EF (2011) Severe,

widespread El Nino associated coral bleaching in the US Phoenix Islands. Bull Mar Sci 87: 623–638.

39. The R Project for Statistical Computing website. Available: http://www.R-project.org/. Accessed 2012 Aug 1.

40. Jolliffe IT (2002) Principal Component Analysis. New York: Springer.

41. MacQueen JB (1967) Some methods for classification and analysis of multivariate observations. Proceedings of 5th Berkeley Symposium on Mathematical Statistics and Probability. University of California Press, Berkeley, CA, USA 1: 281–297.

42. Behrenfeld MJ, Falkowski PG (1997) A consumer's guide to phytoplankton primary productivity models. Limnol Oceanogr 42: 1479–1491.

43. Strickland JDH, Parsons TR (1965) A manual of sea water analysis: with special reference to the more common micronutrients and to particulate organic material. Fish Res Board Can 125: 185.

44. Halpern BS, Walbridge S, Selkoe KA, Kappel CV, Micheli F, et al. (2008) A Global Map of Human Impact on Marine Ecosystems. Science 319: 948–952.

45. Smith VH (2006) Responses of estuarine and coastal marine phytoplankton to nitrogen and phosphorus enrichment. Limnol Oceanogr 51: 377–384.

46. Akaike H (1974) A new look at the statistical model identification. IEEE Transactions on Automatic Control 19:6 716–723.

47. Haas AF, Nelson CE, Wegley-Kelly L, Carlson CA, Rohwer F, et al. (2011) Effects of Coral Reef Benthic Primary Producers on Dissolved Organic Carbon and Microbial Activity. PLoS ONE 6:11 e27973. doi:10.1371/journal.pone.0027973

48. Hopkinson, CS (1985) Shallow-water benthic and pelagic metabolism: evidence of heterotrophy in the nearshore Georgia Bight. Mar Biol 87: 19-32.

49. Hoppe, HG, Gocke, K, Koppe, R, Begler, C (2002) Bacterial growth and primary production along a north–south transect of the Atlantic Ocean. Nature 416: 168–171.

50. Wild, C, et al. (2009) Coral sand O_2 uptake and pelagic–benthic coupling in a subtropical fringing reef, Aqaba, Red Sea. Aquat Biol 6:133–142.

51. Quinones, RA (1992) Size distribution of planktonic biomass and metabolic activity in the pelagic system. PhD Thesis, University of Dalhousie, Canada.

52. Hopkinson, CS, et al. (1989) Size-fractionated metabolism of coastal microbial plankton. Mar Ecol Prog Ser 51: 155-166.

Acknowledgements

Chapter 2, in full, is a reprint of the material as it has been published in PloS ONE. Tracey McDole, James Nulton, Katie Barott, Ben Felts, Carol Hand, Mark Hatay, Hochul Lee, Mark Nadon, Bajador Nosrat, Peter Salamon, Barbara Bailey, Stuart Sandin, Bernardo Vargas-Angel, Merry Youle, Brian Zgliczynski, Rusty Brainard, and Forest Rohwer; 2012. The dissertation author was the primary investigator and author of this paper.

Appendix

Supplemental Figures

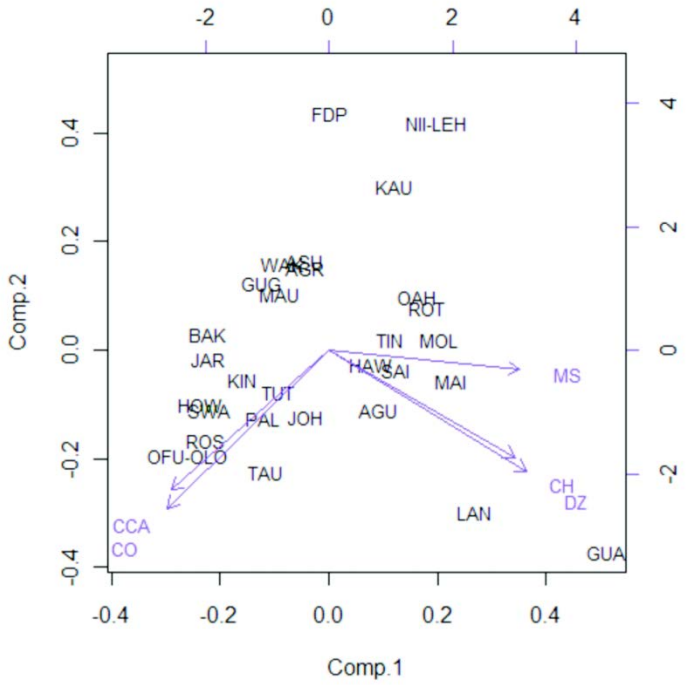

Figure S1. Principal components analysis of reef system properties related to reef health. The first two principal components account for 66% of the variability in the dataset (PC1 = 46%, PC2=20%). Arrow length reflects the relative contribution of a variable to a PC axis. MS = microbialization score; CCA = % crustose coralline algae cover; DZ = % coral disease prevalence; CO = % coral cover; CH = % coral with other indications of compromised health. Symbol denotes oceanographic region: Guam and the Mariana Islands (*), the Main Hawaiian Islands (^), Pacific Remote Islands and Atolls (#), and the Samoa region (+). Two groups of islands identified from k-means cluster analysis are divided along PC1 by the dotted line; the third group is circled (Lanai and Guam). For island abbreviations, see Table 1.

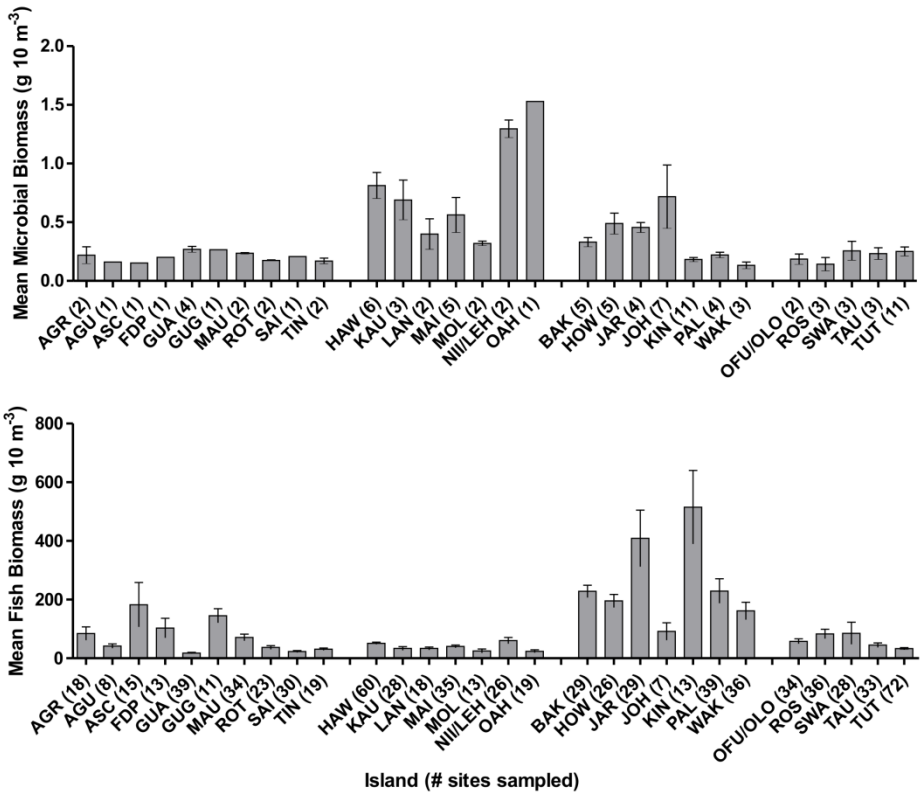

Figure S2. Mean microbial and fish biomass. (a) Mean microbial biomass with standard error. Total number of sites where microbial data was collected = 99. **(b)** Mean fish biomass with standard error. Total number of sites where fish data was collected = 791. The number of REA sites included is given in parentheses next to three-letter island code.

Supplemental Tables

Table S1. Comparison of mean MTE-based microbial metabolic rate predictions from this study with experimental measurements from marine systems[48-52]. Rates of photosynthesis were converted from units of gross carbon production (P_g) to units of power (W) using 39,444 J g^{-1} C, the standard free energy change from the synthesis of glucose from CO_2 and H_2O during photosynthesis at STP[6]. For conversion between rates of oxygen consumption or production in volume or mass units, we assumed that 1 ml O_2 per second = 1.43 mg O_2 per second[24]. To convert between units of power (W) and rates of respiration we assumed that 1W = 0.05 ml O_2 per second[24]. Metabolic rates in W per 10 m^3 were derived after calculating total daily energy use: P_g (from sunrise to sunset) + Respiration (over a 24 hour period). In studies where only dark incubation experiments were performed, total daily energy use was calculated assuming $P_g/R_{24\ hrs} = 1$. When two measurements are listed for the same sample and conditions, they indicate high and low values. B = predicted basal metabolic rate; A = predicted active metabolic rate.

Reference	Microbe Source	Temp (°C)	Method	Habitat type	W per 10 m^3
Hopkinson, C.S. (1985)	water column	10	incubation	nearshore/estuarine	0.4290
		28			2.2663
Hoppe, H.G. *et al.* (2002)	water column	10-20	incubation	N. Atlantic Ocean (30')	0.0131
					0.9861
Wild, *et al.* (2009)	water column	20-28	incubation	reef	0.1298
					1.2508
Quinones, R. (1992)	water column (125 μm -8 mm)	NA	incubation	oceanic shelf	0.0301
	water column (1-125 μm)				0.1483
Hopkinson, C.S., *et al.* (1989)	water column (< 208 μm)	above 20	incubation	open ocean	0.7770
	water column (< 10 μm)				0.6216
	water column (< 1 μm)				0.7382
This study	water column (0.2-10 μm)	27-29	Metabolic Theory of Ecology	reef	0.0002 (B)
					0.1041 (B)
					0.0022 (A)
					2.1412 (A)

Table S2. Summary table showing the number of REA sites where microbial or fish data (belt transect method only) was collected, time period of sampling, and standard error for biomass and abundance of the fish and microbial communities at each island.

REGION: ISLAND or ATOLL		Fish Data			Microbial Data		
Island Code	**Island**	**Stations completed (2001-2009)**	**SEM Total Biomass (all species combined)**	**SEM Abundance (all species combined)**	**Sites sampled (year)**	**SEM Biomass**	**SEM Abundance**
GUAM & MARIANA ISLANDS (orange)							
AGR	Agrihan	18	22.608	0.7211	2 (2009)	0.072	8.65E+04
AGU	Aguijan	8	7.190	0.9009	1 (2009)		
ASC	Asuncion	15	75.603	1.3872	1 (2009)		
FDP	Farallon de Pajaros	13	33.346	0.4974	1 (2009)		
GUA	Guam	39	2.505	0.1451	4 (2009)	0.025	2.96E+04
GUG	Guguan	11	23.890	1.1377	1 (2009)		
MAU	Maug	34	11.502	0.4271	2 (2009)	0.006	4.45E+04
ROT	Rota	23	6.423	0.5365	2 (2009)	0.004	4.50E+04
SAI	Saipan	30	3.333	0.2494	1 (2009)		
TIN	Tinian	19	3.906	0.2538	2 (2009)	0.024	5.40E+04
MAIN HAWAIIAN ISLANDS (MHI, blue)							
HAW	Hawaii	60	3.785	0.2345	6 (2008)	0.111	7.00E+04
KAU	Kauai	28	6.186	0.3308	3 (2008)	0.167	5.01E+04
LAN	Lanai	18	5.138	0.2924	2 (2008)	0.131	9.41E+04
MAI	Maui	35	4.601	0.1926	5 (2008)	0.150	1.74E+04
MOL	Molokai	13	6.576	0.2321	2 (2008)	0.023	1.95E+04
NII/LEH	Niihau & Lehua	26	10.550	0.7855	2 (2008)	0.073	7.54E+04
OAH	Oahu	19	5.038	0.2735	1 (2008)		
PACIFIC REMOTE ISLANDS & ATOLLS (PRIA, pink)							
BAK	Baker	29	20.960	2.3117	5 (2010)	0.040	4.41E+04
HOW	Howland	26	22.573	4.6728	5 (2010)	0.089	3.74E+04
JAR	Jarvis	29	96.484	4.6592	5 (2010)	0.042	5.39E+04
JOH	Johnston	7	29.610	0.4953	5 (2010)	0.270	6.79E+04
KIN	Kingman	13	125.195	1.0118	5 (2010)	0.018	2.25E+04
PAL	Palmyra	39	41.629	0.5140	5 (2010)	0.024	4.01E+04
WAK	Wake	36	29.796	0.2550	5 (2010)	0.028	2.44E+04
SAMOA REGION (green)							
OFU/OLO	Ofu & Olosega	34	8.463	0.3801	5 (2010)	0.044	4.50E+04
ROS	Rose	36	15.827	0.4691	6 (2010)	0.056	5.15E+04
SWA	Swains	28	37.826	0.6721	7 (2010)	0.080	1.84E+04
TAU	Tau	33	7.549	0.2366	8 (2010)	0.051	4.30E+04
TUT	Tutuila	72	3.423	0.2015	9 (2010)	0.039	3.60E+04

Table S3. **Summary table for Figure S1.** The importance of each component and the contribution (loadings) of each variable is shown. MS = microbialization score; CCA = % crustose coralline algae cover; DZ = % coral disease prevalence; CO = % coral cover; CH = % coral with other indications of compromised health.

	Importance of Components				
	Comp.1	*Comp.2*	*Comp.3*	*Comp.4*	*Comp.5*
Standard deviation	1.510	1.003	0.903	0.724	0.613
Proportion of Variance	0.456	0.201	0.163	0.105	0.075
Cumulative Proportion	0.456	0.657	0.820	0.925	1.000
	PCA Loadings				
DZ	0.493	-0.454	0.149	0.394	0.611
CH	0.464	-0.402	-0.504		-0.602
CCA	-0.392	-0.525	0.578	0.283	-0.397
CO	-0.403	-0.593	-0.348	-0.521	0.305
MS	0.475		0.519	-0.697	-0.114

CHAPTER 3

Microbial-mediated resilience on intermediately disturbed coral reefs

Abstract

Microbialization describes the process where micro-organisms, relative to macro-organisms, become increasingly metabolically dominant in an ecosystem. We previously documented microbialization occurring on Pacific coral reef ecosystems where increased algal-derived organic carbon resulting from overfishing and/or eutrophication fuels microbial growth. In this study, we further examine the process of microbialization by assessing the relative energetic contributions of heterotrophic versus autotrophic microbes across 29 Pacific islands experiencing a range of human impacts and oceanographic conditions. Energy flux rates (W 10 m^{-3}) for both groups of microbes were derived allometrically and compared relative to each other. We found that while heterotrophic microbes dominated in terms of biomass (g 10 m^{-3}) microbial autotrophs dominated in terms of energy flux. The ratio of autotrophs to heterotrophs increased with human impact and reef systems experiencing more human impact supported less microbial biomass per unit of energy flux (g W^{-1}). This suggests that autotrophic microbes facilitate the "burning" of excess energy without a corresponding increase in microbial abundance. Autotrophs are also generally less pathogen-like. Together these results show that shifting energy to autotrophic microbes may be an important resilience mechanism for dampening the effects of overfishing and eutrophication on reefs experiencing intermediate levels of microbialization.

Introduction

Aquatic communities are often strongly body size-structured, with most predators larger and less abundant than their prey [1, 2]. These two variables, (size and abundance) help establish the energetic architecture of ecosystems since food webs are networks of pathways for energy flow [3-7]. In oceanic systems including coral reef food webs, the largest pathways for energy and materials flux are typically through the smallest and most abundant organisms, namely the microbes [8-10]. For example, oceanic phytoplankton represent less than half of one percent of the global primary producer biomass, but are responsible for roughly half of the total net primary production (NPP) on the planet [11-13].

Due to their high mass-specific metabolic requirements and rapid biomass turnover, small increases in microbial biomass have a proportionately greater impact on the rate of energy and materials flux than large reductions in fish biomass. For example, to perform work and drive the cellular processes required for life (i.e. biosynthesis, membrane transport, etc.) 1 gram of microbes expends approximately as much energy per unit time as 500 grams of fish [14]. Recently we proposed a metric of reef system health called the *microbialization score;* the total amount of energy required by the microbes divided by the total amount of energy fluxing through the fish in a 10 m^3 column of water [14, 15]. Using this approach, it was shown that microbialization and human impact are strongly correlated on Pacific coral reefs. In

the most heavily impacted reef systems, microbial metabolic rates were up to 100 fold higher than on relatively pristine reef systems [14].

Energy flux rates on coral reefs may be affected by changes in microbial biomass and trophic structure. In addition to human impact driving the benthos to become more autotrophic in nature (i.e., algae replacing corals) [16, 17], there is evidence that on “intermediately disturbed” coral reef systems the microbial community in the water column also shifts towards increased autotrophy. For example, Dinsdale et al. (2008) documented an increase in the relative proportion of autotrophs in the reef water-column along an increasing gradient of human activity (Kingman<Palmyra<Fanning). At the most impacted atoll, Christmas (Kiritimati), there was a switch to an almost pure heterotrophic community containing many potential pathogens. This switch was correlated with the removal of fish herbivores which typically graze on benthic reef algae [19]. Algal-derived dissolved organic matter (DOM) has been shown to directly stimulate the growth of heterotrophic microbes in coral reef systems [20-23], while benthic reef algae [24, 25] and phytoplankton biomass [26, 27] have been shown to respond positively to inorganic nutrient loading.

In this study, energy flux rates for water-column associated autotrophic and heterotrophic microbial compartments were predicted using Metabolic Theory of Ecology or MTE [3, 28]. MTE is based on a mathematical equation which predicts

individual metabolic rate (*I*) from the combined effects of body mass (*M*) and temperature (T). Equation 1 describes the effects of body mass and temperature on whole organism metabolic rate:

$$I = i_0 M^{\alpha} e^{-E/kT} \qquad \text{(Equation 1)}$$

where i_o is the mass-independent normalization constant, *M* is the wet weight of the organism in grams, and α is the scaling exponent. The effects of temperature on metabolic rate are accounted for by $e^{-E/kT}$ [21, 23] where E is the activation energy, *k* is Boltzmann's constant (8.62×10^{-5} eV K^{-1}), and *T* is the water temperature at the site at the time of collection (in Kelvin). The negative sign (in front of E) means that as this ratio decreases, metabolic rate increases (Eq. 1). Therefore, increasing the temperature (T) and/or reducing E will speed up the rate of reaction; the average energy of activation for respiration is ~ 0.65 eV [3], while the effective activation energy for the light reactions of photosynthesis is ~ 0.32 eV [29]. Therefore, at constant temperature and mass, an individual microbe would expend more energy (J s^{-1}) during photosynthesis than respiration. Because this parameter (E) occurs in the exponent (Eq. 1), anthropogenic activities which impact microbial trophodynamics (i.e. alter the ratio of autotrophic to heterotrophic biomass) can significantly alter the system dynamics in terms of energy and materials use.

Here we predict the amount of energy required per unit time in a 10 m^3 column

of reef water (Js^{-1} or W 10 m^{-3}) by the micro and picophytoplankton (< 20 uM) and heterotrophic microbes. We found a highly significant positive relationship between the relative fraction of energy used by the microbial autotrophs and the NCEAS human impact score. Based on these results we argue that the microbial food web is providing a previously uncharacterized mechanism of resilience to moderate some key anthropogenic stressors.

Materials and Methods

Site descriptions: The twenty-nine islands included in this study were surveyed following the National Oceanic and Atmospheric Association (NOAA)'s Rapid Ecological Assessment (REA) protocol as part of the Coral Reef Ecosystem Division (CRED) and Pacific Reef Assessment and Monitoring Program (Pacific RAMP) [30, 31]. Multiple sites (depth: 10-15 m) were sampled at each island in four broad regional groups during the 2008-2010 Pacific RAMP monitoring cruises: the Main Hawaiian Islands (2008), Guam and the Mariana Islands (2009), the American Samoa region (2010), and the Pacific Remote Island Areas (2010). At each site, samples were collected for both flow cytometric analysis as well as metabolic rate predictions (i.e., DAPI stains for size and abundance). Benthic surveys were conducted on the same set of cruises but island-level averages for benthic percent cover data includes sites where microbial data was not collected.

Sample collection/preparation: Seawater samples for flow cytometry were collected approximately 1 m above the reef benthos and processed within 3 hours of collection. Samples were passed through a 20 μm pore size filter (Whatmann) and the filtrate, containing micro and picoautotrophs, was collected. 1 ml aliquots were fixed in EM grade glutaraldehyde (0.125% final concentration; Electron Microscopy Sciences, Hatfield, PA, USA), incubated for 15 minutes at room temperature in the dark, frozen in liquid nitrogen, and stored at -80°C.

On the day of flow cytometry analysis, samples were thawed at 37 °C (samples were only freeze/thawed once) and immediately split into 2 x 500 μl aliquots. One 500 μl aliquot was left unstained and used to report the abundance of micro and picophytoplankton. The other aliquot was stained with SYBR Green I and used to analyze the total number of microbes in each sample (10X final concentration; Invitrogen Molecular Probes, Carlsbad, CA, USA) [32].

Analysis: Samples were analyzed using a BD FACSCanto with a high throughput sampler (HTS) (Becton Dickinson Biosciences, San Jose, CA, USA). One hundred μl of total volume was run at 3 μl sec^{-1}. As a reference, yellow-green fluorescent microspheres (0.75 μm) (Polysciences; Warrington, PA, USA) were added to all samples to ensure that the instrument was stable and to serve an internal verification for sample volume run. Additionally, a previously frozen seawater sample collected off Scripps Pier, La Jolla, CA was also included in every run as a “standard”

to check for consistency between 96-well plate runs. The ratio of autotrophic to heterotrophic microbes was consistent among the La Jolla standard seawater samples for all 96-well plate runs included in the analysis (n = 5, mean = 0.061, SD = 0.006). For the unstained aliquot (autotrophic counts) the threshold was set to chlorophyll fluorescence (red), while the SYBR stained aliquot was acquired with a threshold set to SYBR fluorescence (green). In both cases, the threshold was set by running a sample of molecular grade water (Sigma-Aldrich), and raising threshold just above (or at) the level of noise (Supplementary Figure 1). Samples were excited using a blue laser line (488 nm). For the detection of SYBR fluorescence (total bacteria), a PMT with a 530/30 bandpass filter was used. For the detection of autotrophs, a channel for chlorophyll (back to back LP mirrors resulting in a range of 675-735 nm) and a channel for phycoerytherin (585/42 bandpass filter) were used. Not all of the *Prochlorococcus* cells were quantified because dimly fluorescing cells were below the noise level. Data (.fcs) files were analyzed using FlowJo 7.6.5 software (Treestar Inc., Ashland Oregon). To determine counts of heterotrophic microbes, the autotrophic counts from the non-stained portion were subtracted from the SYBR-stained total count. For each site, relative abundance was calculated by dividing the autotrophic count by the SYBR-stained total count. Relative abundances were then averaged to the island-level.

Calculating autotrophic and heterotrophic energy use: Site-level metabolic rate predictions for all microbes present in a standard volume of water (10 m^3) were

obtained using the methodology described in McDole et al., 2012. These values were averaged to obtain island-level microbial metabolic rates for the 29 islands included in this study. The average energy of activation (E) for respiration (0.61 eV) was used to predict metabolic rates of the heterotrophic microbes [28]. The effective activation energy for the light reactions of photosynthesis is 0.32 eV [29]. A recent transcriptome study in *Prochlorococcus* spp. showed that these two activities have opposite expression patterns relative to the light-dark cycle [33]. Therefore, an average value of 0.46 eV was used to predict metabolic rates for the autotrophic fraction. The predicted scaling exponent (α) used for both trophic components was 1.72 (basal) [28]. Autotrophic energy use was estimated by multiplying the mean ratio of autotrophic cells/total cells measured using flow cytometry by the total predicted microbial power requirements for each island (calculated using only the left side of Equation 1; $i_0 M^{\alpha}$). Heterotrophic energy use was then calculated by subtracting autotrophic energy use from the total predicted microbial power requirements. These values were then multiplied by the right side of Equation 1 ($e^{-E/kT}$) using the respective values for the energy of activation (E).

Quantification of human impact: The level of human impact was assessed from the cumulative global human impact map generated by the National Center for Ecological Analysis and Synthesis (NCEAS; http://www.nceas.ucsb.edu/globalmarine/impacts). Mean impact scores were calculated in ArcGIS 9.3 using previously described methods [14]. These scores

incorporate data related to: artisanal fishing; demersal destructive fishing; demersal non-destructive, high-bycatch fishing; demersal non-destructive low-bycatch fishing; inorganic pollution; invasive species; nutrient input; ocean acidification; benthic structures (e.g., oil rigs); organic pollution; pelagic high-bycatch fishing; pelagic low-bycatch fishing; population pressure; commercial activity (e.g., shipping); sea surface temperature; and ultraviolet insolation.

Estimation of net primary production: Productivity estimations were derived from Moderate Resolution Imaging Spectroradiometer (MODIS) satellite data using the Vertically Generalized Production Model (VGPM; http://www.science.oregonstate.edu/ocean.productivity/standard.product.php). This model, based on an algorithm by Behrenfeld and Falkowski (1997) calculates net primary production from satellite-based measurements of surface chlorophyll a concentrations, while also taking into daily photosynthetically active radiation, and a temperature-dependent photosynthetic efficiency factor. Since these satellite data sets are less accurate for near-shore measurements, the satellite-based NPP values used here were estimated from the data for a 50 km radius ring surrounding each island, with the first 10 km around each island removed.

Water chemistry: At each REA site (~10-15 m depth) diver-deployable 2 L Niskin bottles were filled with water from approximately 1m above the reef benthos. Plastic scintillation vials were rinsed 3X with the water sample before being filled

(200 ml) for nutrient analysis. These samples were stored frozen at -20 degrees C until analysis. Concentrations of nitrite, nitrate, and phosphate were analyzed at NOAA's Pacific Marine Environmental Laboratory (PMEL) (Detection limits: NO_x, 0.01 µM; PO_4^{3-}, 0.01µM).

Results

Links between human activity and trophic structure of the microbial community: The relative abundance of micro and picoautotrophs (i.e. microbial autotrophs) in reef-water was significantly positively correlated with the NCEAS cumulative human impact score (linear regression analysis: n = 29, y = 1.89 x – 6.0, r^2 = 0.46; Pearson correlation: P < 0.0001; Figure 1). In two regions of the study, the highest proportion of microbial autotrophs also occurred on the most impacted islands; Guam in the Mariana Islands, (NCEAS score = 13.7) and Tutuila in the Samoa region (NCEAS score = 12.4) (Figure 1, Supplementary Table 1). This result suggests that increasing human activities on Pacific coral reefs systematically shift the competitive balance between microbial heterotrophs and autotrophs in favor of autotrophs. Surprisingly, the relative proportion of the microbial autotrophs was not correlated with satellite-derived primary productivity (Spearman r: r = 0.31, n=29, P = 0.09, 95% CI = -0.07 to 0.62; Supplementary Table 2).

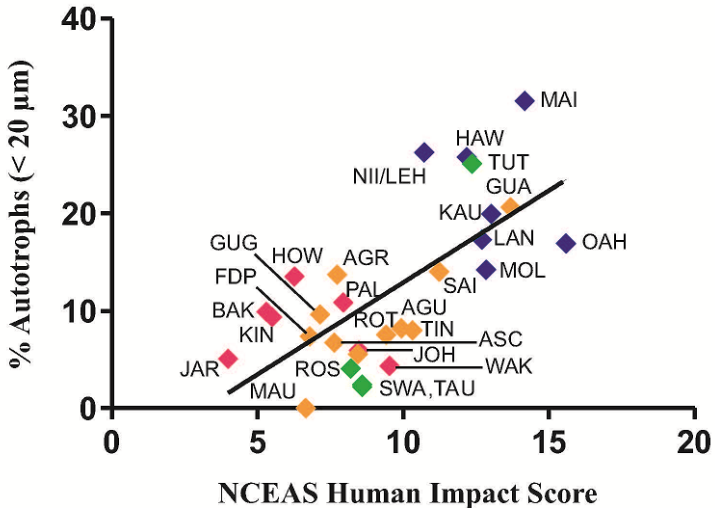

Figure 3.1. The relationship between the island-level NCEAS cumulative human impact scores and the autotrophic fraction of the microbial community (< 20 um; micro and picoautotrophs) (Linear regression analysis: n=29, y= 1.89 x – 6.0, r^2 = 0.46, Pearson r: P < 0.0001). Color denotes oceanographic region: Guam and the Mariana Islands (orange circles), the Main Hawaiian Islands (blue circles), Pacific Remote Islands Areas (pink circles), and American Samoa (green circles). For 3-letter island codes, see Table 1.

Table 3.1. Three-letter codes for islands surveyed, grouped by region. Colors identify each regional island group in the figures.

REGION: ISLAND or ATOLL	
Island Code	**Island**
GUAM & MARIANA ISLANDS (orange)	
AGR	Agrihan
AGU	Aguijan
ASC	Asuncion
FDP	Farallon de Pajaros
GUA	Guam
GUG	Guguan
MAU	Maug
ROT	Rota
SAI	Saipan
TIN	Tinian
MAIN HAWAIIAN ISLANDS (MHI, blue)	
HAW	Hawaii
KAU	Kauai
LAN	Lanai
MAI	Maui
MOL	Molokai
NII/LEH	Niihau & Lehua
OAH	Oahu
PACIFIC REMOTE ISLAND AREAS(PRIA, pink)	
BAK	Baker
HOW	Howland
JAR	Jarvis
JOH	Johnston
KIN	Kingman
PAL	Palmyra
WAK	Wake
AMERICAN SAMOA (green)	
OFU/OLO	Ofu & Olosega
ROS	Rose
SWA	Swains
TAU	Tau
TUT	Tutuila

Regardless of oceanographic context, larger islands are often more populated. For example, in our 29-island dataset, NCEAS human impact scores are highly correlated with log land area (km^2) (linear regression analysis: n = 29, y = 1.98 x – 6.7, $r^2 = 0.70$; Pearson correlation: $P < 0.0001$). Island size could be confounding the positive correlation between the level of human impact and the percent autotrophs (Figure 1). To address this issue, land area (km^2) and reef area (km^2) were included as possible predictor variables in multiple linear regression analysis [35]. This resulted in four models of interest: percent autotrophs = $\beta 0 + \beta 1$ (NCEAS), y = $\beta 0 + \beta 1$ (NCEAS) + $\beta 2$ (log land area), y = $\beta 0 + \beta 1$ (NCEAS) + $\beta 2$ (log reef area), y = $\beta 0 + \beta 1$ (NCEAS) + $\beta 2$ (log land area) + $\beta 3$ (log reef area). The regression coefficients (β) represent the relative contribution of each of the independent variables to the prediction of the dependent variable (y), where y = percent autotrophs. In the first model, the NCEAS score was significant, having a p-value less than 0.0001. Using a t-test, and given that the NCEAS score is included in the model, the p-values associated with land area (but not reef area) were significant in both the two and three parameter models (p-value < 0.01). Using a model selection criteria, the model with the smallest AIC value included land area as an additional variable (y = $\beta 0 + \beta 1$ (NCEAS) + $\beta 2$ (log land area) [36]. This model explained 57% of the variability in the percent autotrophs; an improvement over the simplest model (y = $\beta 0 + \beta 1$ (NCEAS)) which explained 45% of the variability. These analyses support the hypothesis that the trophic balance between autotrophs and heterotrophs in reef water is largely driven by the combined effects of human impact and island size rather than oceanographic setting.

To investigate whether anthropogenic-based sources of nutrient input might explain the positive relationship between the relative abundance of phytoplankton and human impact, mean NCEAS layers for nutrient input (based on average annual use of fertilizer) and non-point source inorganic pollution (urban runoff) were obtained from http://globalmarine.nceas.ucsb.edu [37]. In the Marianas islands (n = 5), a strong positive relationship was found between inorganic pollution and the percent of micro and picoautotrophs (linear regression: $y = 213.0\ x + 5.98$, $r^2 = 0.87$, Pearson corr., $P < 0.05$) (Figure S2). By comparison, in the MHI region (n = 7), percent micro and picoautotrophs were not correlated with either inorganic pollution (urban runoff) or nutrient input (fertilizer use). No significant relationships were found between nutrients levels (PO_4^{3-}, SiO_2, or NO_x) and abundance of microbial autotrophs in any of the regions (Table S2).

To examine how changes in microbial trophic structure affect reef microbialization, energy flux rates (W 10 m^{-3}) for both groups of microbes were derived allometrically and compared. A highly significant positive correlation (n = 28, $y = 0.77\ x - 1.86$; $r^2 = 0.80$) was found between the amount of energy fluxed by the heterotrophic microorganisms and that of the photosynthetic micro and picoplankton (Figure 2). This result implies that phytoplankton-bacterioplankton coupling may be described by a power relationship. The slope of the log-log plot is less than unity (slope = 0.77); heterotrophic power requirements increased more slowly than those of the autotrophic component (Figure 2). Assuming that our allometric calculations are

correct, the autotrophic microbes may use up to 128X more energy per second than the heterotrophic microbes. The large difference in energy use per unit area per unit time (W 10 m^{-3}) between the two microbial trophic levels is due to the lower activation barrier required for the light reactions of photosynthesis versus the biochemical reactions of the Calvin cycle (respiration). Thus, at constant temperature and mass, an individual microbe expends more energy (J s^{-1}) during photosynthesis than respiration (Equation 1). Together with Figure 1, these results suggest that anthropogenic activities can alter the competitive balance between autotrophs and heterotrophs and cause dramatic increases in rates of energy and materials flux on impacted coral reefs systems.

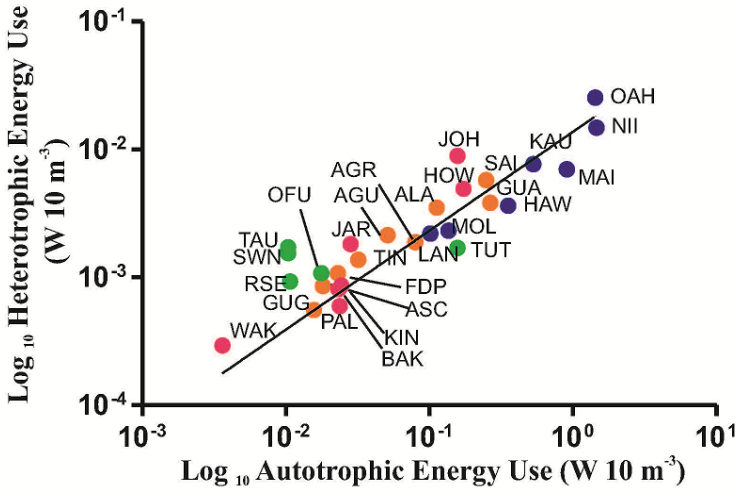

Figure 3.2. Least squares regression analysis on log transformed energy use predictions for autotrophic and heterotrophic components (< 20 μm fraction; micro and picoautotrophs) in the 10^3 water-column above the reef sites (n = 28, y = 0.77 x – 1.86; r^2 = 0.80). Colors represent oceanographic region: Main Hawaiian Islands (blue), Guam & Mariana Islands (orange), Pacific Remote Islands Areas (pink circles), and American Samoa (green circles).

Relative energy flux through the microbial loop by heterotrophic microbes is reduced as total power requirements increase. In the reef water column, heterotrophic microbes were always more abundant than photosynthetic micro and picoplankton (69-98% of the total SYBR + count). Yet their predicted contribution to the total energy use was minor and ranged from 14% around Tau Island in American Samoa to 1% around Maui Island in the Main Hawaiian Islands (Figure 3). This percentage was related to total energy use; as total microbial power requirements increased, heterotrophic microbes had less metabolic significance. In Figure 3, the discontinuous increase in the total amount of energy fluxing through the water-column is largely driven by autotrophic microbes (and their lower energy barrier). A highly significant correlation was found to exist between total predicted energy use (W 10 m^{-3}) and the number of microbial autotrophs (cells ml^{-1}) (Spearman $_{autotrophs}$: r = 0.82, n=27, P = 0.0001, 95% CI = -0.63 to 0.91) but not the number of microbial heterotrophs (Spearman r $_{heterotrophs}$: r = -0.04, n=27, P = 0.83, 95% CI = -0.42 to 0.35).

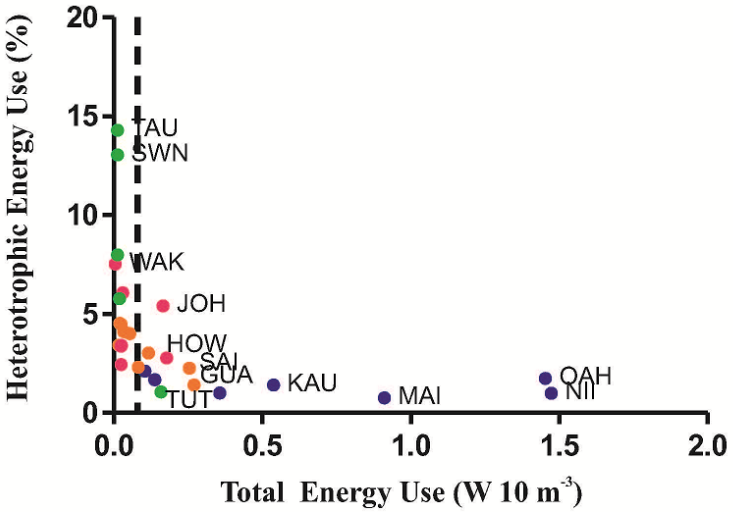

Figure 3.3. The percent of energy used by heterotrophic microbes plotted as a function of total predicted microbial power requirements. The grid line at x = 0.08 W 10 m^{-3} represents the first natural break in the data set identified using the Jenks' Natural Breaks algorithm ([R] statistical package: classIntervals, style: jenks). Colors represent oceanographic region: Main Hawaiian Islands (blue), Guam & Mariana Islands (orange), Pacific Remote Islands Areas (pink circles), and American Samoa (green circles).

In the euphotic zone of the open ocean, i.e. oligotrophic waters, where nutrient supply is thought to limit phytoplankton biomass, bacterial abundance may be close to a lower threshold [38]. Predation by bacterivores and bacteriophage may be less efficient near this lower bound, and the mobilization of nutrients via the microbial loop may be reduced. As previously stated, the proportion of the total energy fluxed by the autotrophic microbes was not correlated with levels of net primary production occurring over 10 km offshore. This may be because as reef systems become more impacted, microbial density increases and predation-driven remineralization processes are more likely to fuel microbialization processes [39, 40].

Using the Jenks' Natural Breaks algorithm in R (http://www.R-project.org), a lower bound for total metabolic rate (the first natural break in the dataset) was identified (Figure 3). This lower bound contained 53% of the entire dataset. Below this lower bound (< 0.08 W 10 m^3), the relative contribution of heterotrophic microbes to total energy use was highly variable (2% -14%). Above this lower bound, the autotrophic to heterotrophic energy flux ratio remained fairly fixed. On 92% of the reefs with total microbial metabolic rate predictions above 0.08 W 10 m^3, heterotrophic microbes accounted for less than 5% of the total energy use predictions. Reefs where total microbial energy use predictions exceed this lower bound (0.08 W 10 m^{-3}) are likely to be experiencing some degree of microbialization. These locations include all of the Main Hawaiian Islands and those islands with the highest NCEAS scores within each respective region: Guam and Saipan (Marianas), Tutuila (American Samoa), and Johnston (PRIAs) (Figure 3).

More human impacted reefs support less microbial biomass per unit of energy flux: In size-structured food webs, inverted biomass pyramids can exist because larger organisms (higher trophic levels) require less energy per gram. Similarly, in the microbial food web, the lowest trophic level (autotrophic microbes) not only has access to a larger pool of available energy, but also a greater ability to dissipate it. This is because at constant temperature and mass, an individual microbe expends more energy (J s^{-1}) during photosynthesis than respiration. To further investigate the bioenergetic role of the microbial component with respect to ecosystem functioning,

the amount of microbial biomass supported per unit of energy degraded (g W^{-1}) was derived by dividing mean microbial biomass (g 10 m^{-3}) by the total microbial metabolic rate predicted for each island (W 10 m^{-3}). When this parameter was plotted as a function of human impact, reef systems with lower NCEAS scores (i.e., less human impact) tended to support a greater amount of microbial biomass (g) per unit of energy flux (W or J s^{-1}) (Figure 4). In other words, the metabolic efficiency of the microbial community decreases with human impact. For example, on Johnston Atoll, the most impacted island in the PRIAs group (NCEAS score = 8.5), 4 grams of microbes in 10 cubic meters of water overlying the reef required 1 joule of chemical energy every second. On Kingman Atoll (PRIAs), one of the least impacted reef systems in the data set (NCEAS score = 5.5), the same amount of energy (1 J s^{-1}) supports twice as much microbial biomass (8 grams). Similarly, in the American Samoa region, the amount of microbial biomass supported per unit of energy flow was reduced from 21 g W^{-1} on Swain's Island (NCEAS score = 8.6) to 1.5 g W^{-1} on Tutuila, the most heavily impacted island in the region (NCEAS score = 12.4) (Figure 4). Within the Marianas group, the most impacted islands (Guam and Saipan) also support the least amount of microbial biomass per unit of energy flux. Significant differences in biomass per unit energy flux were identified between the MHI region and both the PRIAs and American Samoa regions (Kruskall-Wallis: $n = 28$, $P = 0.006$; Dunn's Multiple Comparison: $P < 0.05$ for both regions).

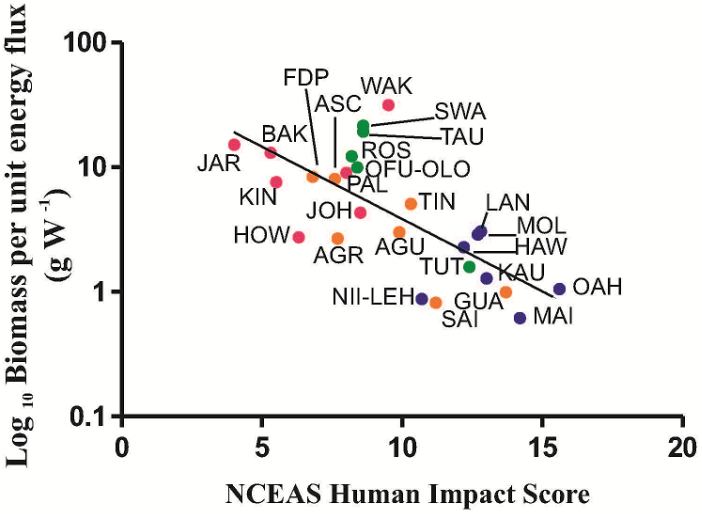

Figure 3.4. The amount of microbial biomass supported per unit of energy flow versus NCEAS cumulative human impact score (n = 26, y = -0.16 x + 1.74; r^2 = 0.50). For each island, biomass per unit energy flux (g W^{-1} 10 m^{-3}) was calculated by dividing total microbial biomass by total predicted metabolic rate. Colors represent oceanographic region: Main Hawaiian Islands (blue), Guam & Mariana Islands (orange), Pacific Remote Islands Areas (pink circles), and American Samoa (green circles).

Discussion

We previously showed that reef microbialization and human impact are highly correlated on Pacific coral reefs [14]. In the Northern Line Islands, metagenomic analysis showed an increase in the relative fraction of autotrophic microbes concurrent with an increase in microbial counts (fluorescent microscopy) across an increasing gradient of human disturbance [18]. In this study, FACS analysis showed similar trends occurring on both regional and Pacific-wide scales. Increased microbial abundances with increasing human impact have also been documented in Brazil [41] and Sri Lanka [42]. Here we have extended this data and shown that the microbial autotrophs are predicted to play disproportionately large metabolic roles on

"intermediately disturbed" coral reefs. The energetic predictions for our 29-island dataset suggest that the microbial ecology of these locations is not yet "extremely degraded", e.g. Christmas (Kiritimati) atoll, where the microbial community is dominated by heterotrophs containing many potential pathogens [18].

One mechanism thought to stimulate the rise of opportunistic pathogens and facilitate coral to algal phase shifts is the microbial-mediated DDAM feedback model (Dissolved Organic Carbon, Disease, Algae, and Microbes) [43, 44]. In the DDAM model, reduced grazing by herbivores (due to overfishing) and/or nutrient additions stimulate the growth of fleshy algae (macroalgae and turf algae) which release DOC, a source of carbon almost exclusively available to heterotrophic microbes including opportunistic pathogens (microbes that are normally present within the environment but may opportunistically become causative agents of coral disease) [43]. Disease outbreaks and coral death result in more free space available for DOC-producing fleshy algae.

In general, autotrophic microbes are much less likely to be potential coral pathogens. Anthropogenic activities that result in more energy and materials being shunted towards microbial autotrophs rather than heterotrophs could potentially suppress the rise of opportunistic pathogens. We hypothesize that this type of shift may actually buffer reefs from anthropogenic influences and contribute to coral reef resilience; higher metabolic demands allow for rapid turnover and processing of

excess energy and materials without a corresponding increase in the number of disease-causing agents. A key finding from this analysis in support of this hypothesis is that as Pacific coral reefs become more impacted, the microbial community becomes less efficient overall in terms of conversion of energy into organic structure. The "burning" of excess energy dampens the effect that human impact might otherwise have on microbial biomass. It may be only in the severely degraded state (e.g. Christmas atoll) that the relative competitiveness of autotrophic microbes becomes reduced, and the dominant controlling feedback shifts from intermediate microbialization to DDAM feedback (where heterotrophic pathways of energy flow are reestablished through super-heterotrophic microbes, bacteria that live in extremely energy-rich environments with more pathogen-like or copiotrophic growth strategies).

In conclusion, the results of this study are consistent with the DDAM model. However, this study suggests a new relationship between microbialization and reef system functioning: microbialization as a resilience mechanism. Higher relative energy flux by autotrophic microbes may reduce the rate at which a coral reef moves towards an alternative stable state in response to human impact. Thus, intermediate microbialization may promote continuous (as opposed to discontinuous) phase shift, which would ultimately make it easier for a reef system to return to the “original” and/or a less-degraded state [45].

References

1. Sheldon, R. W., Sutcliffe Jr., W. H. & Paranjape, M. A. 1977 Structure of Pelagic Food Chain and Relationship Between Plankton and Fish Production. *J. Fish. Res. Board Can.* **34**, 2344–2353.

2. Jennings, S. 2005 Size based analysis of aquatic food webs. In *Aquatic Food Webs: An Ecosystem Approach*. (ed. Belgrano, A, Scharler, U.M., Dunne, J., Ulanowicz, R.E.), pp. 87-97. USA: Oxford University Press.

3. Brown JH, Gillooly JF, Allen AP, Savage VM, West GB 2004 Toward a metabolic theory of ecology. *Ecology* **85**, 1771–1789.

4. White, E. P., Ernest, S. K. M., Kerkhoff, A. J. & Enquist, B. J. 2007 Relationships between body size and abundance in ecology. *Trends Ecol. Evol.* **22**, 323–330.

5. Jennings, S. & Mackinson, S. 2003 Abundance–body mass relationships in size-structured food webs. *Ecol. Lett.* **6**, 971–974.

6. Ackerman, J. L., Bellwood, D. R. & Brown, J. H. 2004 The contribution of small individuals to density-body size relationships: examination of energetic equivalence in reef fishes. *Oecologia* **139**, 568–571.

7. Belgrano, A., Allen, A. P., Enquist, B. J. & Gillooly, J. F. 2002 Allometric scaling of maximum population density: a common rule for marine phytoplankton and terrestrial plants. *Ecol. Lett.* **5**, 611–613.

8. Hagström, A., Azam, F., Andersson, A., Wikner, J. & Rassoulzadegan, F. 1988 Microbial loop in an oligotrophic pelagic marine ecosystem: possible roles of cyanobacteria and nanoflagellates in the organic fluxes. *MEPS* **49**, 171–178.

9. Rivkin, R. B. & Legendre, L. 2001 Biogenic Carbon Cycling in the Upper Ocean: Effects of Microbial Respiration. *Science* **291**, 2398–2400.

10. Dick Van Oevelen, K. S. 2006 Carbon flows through a benthic food web: Integrating biomass, isotope and tracer data. *J. Mar. Res.* **64**, 453–482.

11. Longhurst, A., Sathyendranath, S., Platt, T. & Caverhill, C. 1995 An estimate of global primary production in the ocean from satellite radiometer data. *J. Plankton Res.* **17**, 1245–1271

12. Antoine, D., André, J.-M. & Morel, A. 1996 Oceanic primary production: 2.

Estimation at global scale from satellite (Coastal Zone Color Scanner) chlorophyll. *Global Biogeochem. Cycles* **10**, 57–69.

13. Field, C. B., Behrenfeld, M. J., Randerson, J. T. & Falkowski, P. 1998 Primary Production of the Biosphere: Integrating Terrestrial and Oceanic Components. *Science* **281**, 237–240

14. McDole, T., Nulton, J., Barott, K.B., Felts, B., Hand, C., Hatay, M., Lee, H., Nadon, M.O., Nosrat, B., Salamon, P., *et al.* 2012 Assessing Coral Reefs on a Pacific-Wide Scale Using the Microbialization Score. *PLoS ONE* **7**, e43233.

15. Jackson J.B.C., Kirby M.X., Berger W.H., Bjorndal K.A., Botsford L.W., Bourque, B.J., Bradbury, R.H., Cooke, R., Erlandson, J., Estes, J.A., et al. 2001 Historical overfishing and the recent collapse of coastal ecosystems. *Science* **293**, 629.

16. Bruno, J. F., Sweatman, H., Precht, W. F., Selig, E. R. & Schutte, V. G. W. 2009 Assessing evidence of phase shifts from coral to macroalgal dominance on coral reefs. *Ecology* **90**, 1478–1484.

17. Kelly, L. W., Barott, K.L., Dinsdale, E., Freidlander, A.M., Nosrat, B., Obura, D., Sala, E., Sandin, S.A., Smith, J.E., Vermeij, M.A., *et al.* 2011 Black reefs: iron-induced phase shifts on coral reefs. *ISME* J (10.1038/ismej.2011.114)

18. Dinsdale, E., Pantos, O., Smriga, S. & Edwards, R. 2008 Microbial ecology of four coral atolls in the Northern Line Islands. *PLoS One* **3(2),** e1584 (doi:10.1371/journal.pone.0001584)

19. Sandin S.A., Smith J.E., DeMartini E.E., Dinsdale E.A., Donner S.D., Freidlander, A.M., Konotchick, T., Malay, M., Maragos, J.E., Obura, D., *et al.* 2008 Baselines and degradation of coral reefs in the Northern Line Islands. *PLoS ONE* **3(2)**, e1548 (doi:10.1371/journal.pone.0001548)

20. Smith, J. E., Shaw, M., Edwards, R.A., Obura, D., Pantos, O., Sala, E., Sandin, S.A., Smriga, S., Hatay, M., Rohwer, F. 2006 Indirect effects of algae on coral: algae-mediated, microbe-induced coral mortality. *Ecol. Lett.* **9**, 835–845.

21. Haas, A. F., Naumann, M.S., Struck, U., Mayr, C., el-Zibdah, M., Wild, C. 2010 Organic matter release by coral reef associated benthic algae in the Northern Red Sea. *J. Exp. Mar. Biol. Ecol.* **389**, 53–60.

22. Haas, A. F., Nelson, C.E., Wegley Kelly, L., Carlson, C.A., Rohwer, F., Leichter, J.A., Wyatt, A., Smith, J.E. 2011 Effects of Coral Reef Benthic Primary Producers on Dissolved Organic Carbon and Microbial Activity. *PLoS*

ONE **6**, e27973 (10.1371/journal.pone.0027973)

23. Wild, C., Niggl, W., Naumann, M. S. & Haas, A. F. 2010 Organic matter release by Red Sea coral reef organisms—potential effects on microbial activity and in situ O_2 availability. *Mar. Ecol. Prog. Ser.* **411**, 61–71.

24. Vermeij, M. J. A. van Moorselaar, I., Engelhard, S., Hörnlein, C., Vonk, S.M., Visser, P.M. 2010 The Effects of Nutrient Enrichment and Herbivore Abundance on the Ability of Turf Algae to Overgrow Coral in the Caribbean. *PLoS ONE* **5(12)**, e14312 (10.1371/journal.pone.0014312)

25. Fabricius, K. E. 2011 Factors Determining the Resilience of Coral Reefs to Eutrophication: A Review and Conceptual Model. In *Coral Reefs: An Ecosystem in Transition* (ed. Dubinsky, Z., Stambler, N.) pp. 493–505. Springer Netherlands.

26. Smith, V. H. 2006 Responses of estuarine and coastal marine phytoplankton to nitrogen and phosphorus enrichment. *Limnol. Oceano.* **51**, 377-384.

27. Brodie, J.E., Devlin, M., Haynes, D. & Waterhouse, J. 2011 Assessment of the eutrophication status of the Great Barrier Reef lagoon (Australia). *Biogeochemistry* **106**, 281-302.

28. DeLong J.P., Okie J.G., Moses M.E., Sibly R.M., & Brown J.H. 2010 Shifts in metabolic scaling, production, and efficiency across major evolutionary transitions of life. *Proc Natl Acad Sci USA* **107**, e12941

29. Allen, A., Gillooly, J. & Brown, J. 2005 Linking the global carbon cycle to individual metabolism. *Funct. Ecol.* **19**, 202–213.

30. Brainard, R., Asher J., Gove J., Helyer J., Kenyon J., Mancini F., Miller J., Myhre S., Nadon M., Rooney J., *et al.* 2008 Coral Reef Ecosystem Monitoring Report for American Samoa: 2002 – 2006, NOAA Special Report NMFS PIFSC, Honolulu, HI pp. 510

31. Brainard R.E., Asher J., Blyth-Skyrme V., Coccagna E.F., Dennis K., Donovan M.K., Gove J.M., Kenyon J., Looney E.E., Miller J.E. 2012 Coral Reef Ecosystem Monitoring Report for the Mariana Archipelago: 2003 – 2007, NOAA Fisheries, Pacific Islands Fisheries Science Center, PIFSC Special Publication, SP-12-01, pp. 1019

32. Marie, D., Partensky, F., Jacquet, S. & Vaulot, D. 1997 Enumeration and Cell Cycle Analysis of Natural Populations of Marine Picoplankton by Flow Cytometry Using the Nucleic Acid Stain SYBR Green I. *Appl Environ*

Microbiol **63**, 186–193.

33. Zinser, E. R. Lindell, D., Johnson, Z.I., Futschik, M.E., Steglich, C., Coleman, M.L., Wright, M.A., Rector, T., Steen, R., McNulty, N. 2009 Choreography of the Transcriptome, Photophysiology, and Cell Cycle of a Minimal Photoautotroph, Prochlorococcus. *PLoS ONE* **4**, e5135. (10.1371/journal.pone.0005135)

34. Behrenfeld, M. J. & Falkowski, P. G. 1997 A consumer's guide to phytoplankton primary productivity models. *Limnol Oceanogr* **42**, 1479–1491.

35. Gove J.M., G.J. Williams, M.A. McManus, S.F. Heron, S.A. Sandin, O.J. Vetter and and D.G. Foley. submitted. Quantifying climatological ranges and anomaly frequencies for Pacific Island reef ecosystems. *Coral Reefs*.

36. Akaike, H 1974 A new look at the statistical model identification. *IEEE Transactions on Automatic Control* **19(6)**, 716–723.

37. Halpern, B. S., Walbridge, S., Selkoe, K.A., Kappel, C.V., Micheli, F., D'Agrosa, C., Bruno, J.F., Casey, K.S., Ebert, C., Fox, H.E., *et al*. 2008 A Global Map of Human Impact on Marine Ecosystems. *Science* **319**, 948–952.

38. Cho, B. C and Azam, F. 1990 Biogeochemical significance of bacterial biomass in the ocean's euphotic zone. *MEPS* **63**, 253-259.

39. Drakare, S. 2002 Competition between Picoplanktonic Cyanobacteria and Heterotrophic Bacteria along Crossed Gradients of Glucose and Phosphate. *Microb. Ecol.* **44**, 327-335.

40. Danger, M., Leflaive, J., Oumarou, C., Ten-Hage, L. & Lacroix, G. 2007 Control of phytoplankton–bacteria interactions by stoichiometric constraints. *Oikos* **116**, 1079–1086.

41. Bruce, T., Meirelles, P.M., Garcia, G., Paranhos, R., Rezende, C.E., de Moura, R.L., Filho, R., Coni, E.O.C., Vasconcelos, A.T., Amado Filho, G. *et al.* 2012 Abrolhos Bank Reef Health Evaluated by Means of Water Quality, Microbial Diversity, Benthic Cover, and Fish Biomass Data. *PLoS ONE* **7**, e36687 (10.1371/journal.pone.0036687)

42. Fairoz, M.F.M., and Rohwer, F. 2007 Water Chemistry and Coral heath Assessment of Sri Lankan reefs. 21st Pacific Science Congress, Pacific Science Association, 12-18, 2007, November, Okinawa, Japan.

43. Dinsdale, E. A. & Rohwer, F. 2011 Fish or Germs? Microbial Dynamics

Associated with Changing Trophic Structures on Coral Reefs In *Coral Reefs: An Ecosystem in Transition* (ed. Dubinsky, Z. and Stambler, N.) pp. 231–240. Springer Netherlands.

44. Barott, K. L. & Rohwer, F. L. 2012 Unseen players shape benthic competition on coral reefs. *Trends Microbiol.* (doi:10.1016/j.tim.2012.08.004)

45. Fung, T., Seymour, R. M. & Johnson, C. R. 2010 Alternative stable states and phase shifts in coral reefs under anthropogenic stress. *Ecology* **92**, 967–982.

Acknowledgements

Chapter 3, in full, is a reprint of the material as it has been submitted to Proceedings of the Royal Society B: Biological Sciences. Tracey McDole, Brett Hilton, Juris Agrasis, James Nulton, Barbara Bailey, Bajador Nosrat, Chris Sullivan, Mark Hatay, Katie Barrott, Bernardo Vargas-Angel, Rusty Brainard, and Forest Rohwer. The dissertation author was the primary investigator of this paper.

Appendix

Supplementary Figures

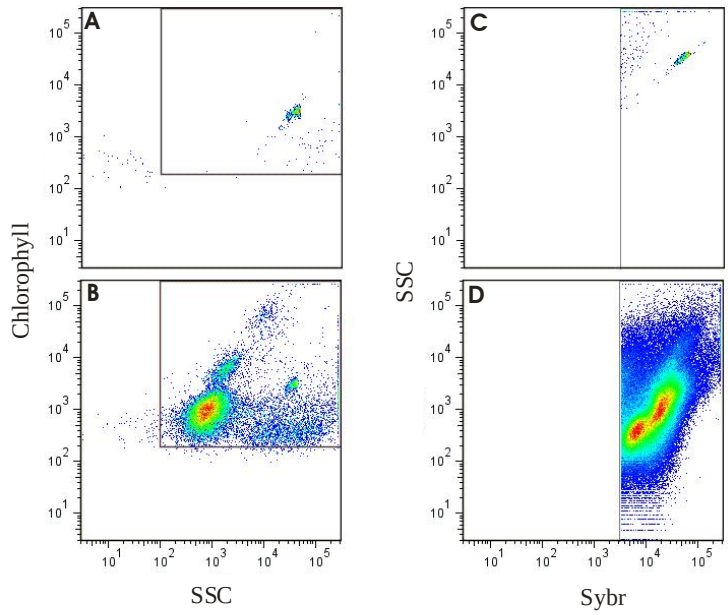

Figure S1. Flow Cytometry Analysis of a representative reef-water sample A) Molecular grade water only (Sigma-Aldrich) with yellow-green fluorescent microspheres (0.75 μm). This was used to verify minimal background with the instrument settings. B) A representative marine sample, run with the same settings and layout as in A. The beads can still be seen in the same location, along with several populations of autotrophs. The gate encompasses all events counted as autotrophic C) The same sample as in B, viewed in the same manner as it will be analyzed for the SYBR Green I stained aliquot. This was used to set the gate for SYBR positive events (autotrophic + heterotrophic count) and minimize background. D) The representative reef-water sample stained with SYBR Green I. The gate set determined the total number of marine microbes in the sample. Heterotrophs were calculated by subtracting the events in the gate of plot B from the events in the gate of plot D.

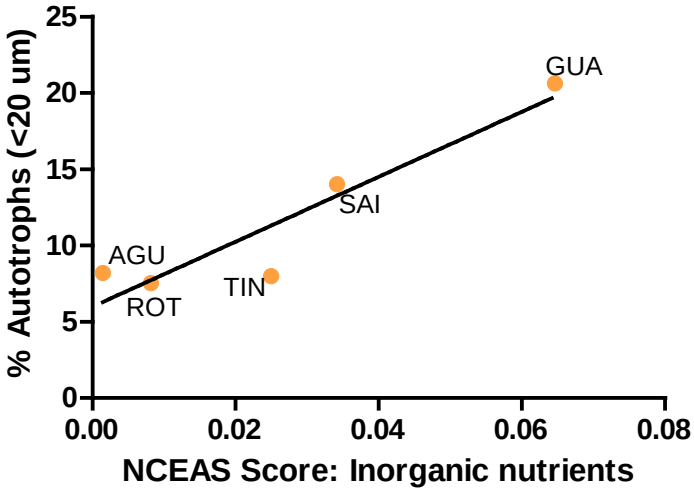

Figure S2. The relationship between the relative abundance of microbial autotrophs and inorganic pollution (urban run-off) in the Marianas region. The data layer for inorganic pollution, extracted from the NCEAS website, returned values for 5 of 10 island locations in the region including the 4 most populated islands (Guam, Saipan, Rota, and Tinian) and one uninhabited island (Aguijan). Linear regression analysis: $y = 213.0\ x + 5.98$, $r^2 = 0.87$.

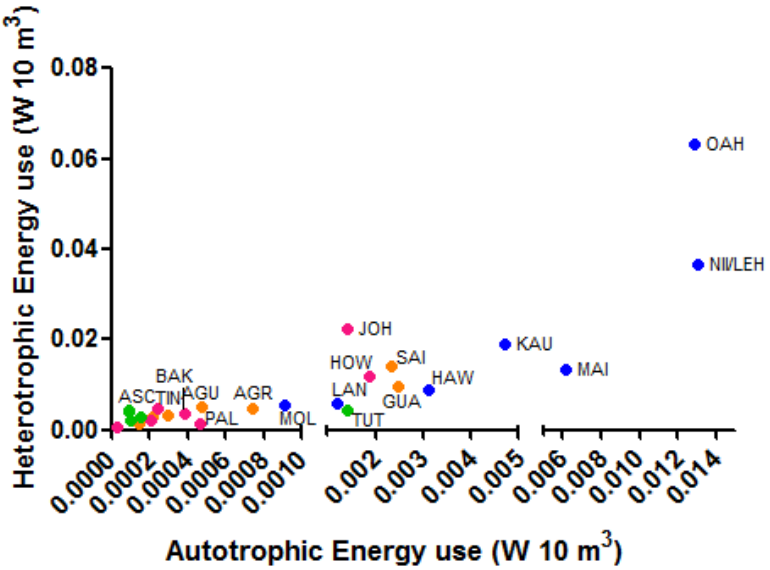

Supplementary Figure S3. The predicted metabolic rates of the water-column associated microbial autotrophs versus the microbial heterotrophs. Autotrophic energy use spans approximately three orders of magnitude while heterotrophic energy use increases by only two orders of magnitude. The x-axis is segmented to improve data visualization.

Supplementary Tables

Table S1. NCEAS cumulative human impact scores shown with the values for the percent of the microbial community that is autotrophic (micro and picophytoplankton). The 29 islands that were included in this study are located in the central and western Pacific, and are grouped by oceanographic region. Values provided for the NCEAS score and the percent autotrophs represent island-level means; STDEV is the standard deviation from this mean for the percent autotrophs.

REGION: ISLAND or ATOLL					
Island Code	**Island**	**NCEAS Impact Score**	**% Autotrophs**	**# Sites**	**STDEV**
GUAM & MARIANA ISLANDS (orange)					
AGR	Agrihan	7.7	13.7	1	na
AGU	Aguijan	9.9	8.2	1	na
ASC	Asuncion	7.6	6.7	2	4.2
FDP	Farallon de Pajaros	6.8	7.4	1	na
GUA	Guam	13.7	20.6	3	8.8
GUG	Guguan	7.1	9.6	1	na
MAU	Maug	6.7	0.0	1	na
ROT	Rota	9.4	7.5	1	na
SAI	Saipan	11.2	14.0	3	3.4
TIN	Tinian	10.3	8.0	2	4.9
MAIN HAWAIIAN ISLANDS (MHI, blue)					
HAW	Hawaii	12.2	25.8	1	na
KAU	Kauai	13.0	19.9	2	5.6
LAN	Lanai	12.7	17.3	2	3.6
MAI	Maui	14.2	31.5	2	3.2
MOL	Molokai	12.8	14.2	2	5.7
NII/LEH	Niihau & Lehua	10.7	26.2	2	16.5
OAH	Oahu	15.6	16.9	2	1.0
PACIFIC REMOTE ISLANDS & ATOLLS (PRIA, pink)					
BAK	Baker	5.3	9.9	4	1.8
HOW	Howland	6.3	13.5	4	5.9
JAR	Jarvis	4.0	5.1	4	2.9
JOH	Johnston	8.5	5.9	5	3.9
KIN	Kingman	5.5	9.3	2	2.8
PAL	Palmyra	8.0	10.8	4	5.7
WAK	Wake	9.5	4.4	5	1.6
SAMOA REGION (green)					
OFU/OLO	Ofu & Olosega	8.4	5.5	2	0.5
ROS	Rose	8.2	4.1	3	1.8
SWA	Swains	8.6	2.4	2	2.2
TAU	Tau	8.6	2.2	2	0.5
TUT	Tutuila	12.4	25.1	2	6.1

Table S2. Complete results table for regional and Pacific-wide correlation analyses. The covariation between the autotrophic fraction of the microbial community and a number of different oceanographic proxies was assessed including: the NCEAS cumulative human impact score, satellite-derived values of net primary production (NPP), and inorganic nutrients (NO_x, PO_4^{3-}, and SiO_2). The number of islands included in the analysis (n), correlation coefficients (r), and 95% confidence intervals are included. Significant correlations (P = 0.05) are in bolded font.

Pacific wide	**NCEAS**	**Pearson r**	**0.7**	**29**	**0.0001**	**0.42 to 0.83**	*******
Marianas			**0.7**	**10**	**0.015**	**0.12 to 0.93**	*****
MHI			-0.2	7	0.647	-0.83 to 0.64	ns
PRIAs			-0.2	7	0.621	-0.83 to 0.63	ns
Samoa			**1.0**	**5**	**0.004**	**0.71 to 0.10**	******
Pacific wide	NPP	Spearman r	0.31	29	0.10	-0.07 to 0.62	ns
Marianas			-0.5	10	0.14	na	ns
MHI			**-0.9**	**7**	**0.01**	**na**	******
PRIAs			0.4	7	0.38	na	ns
Samoa			0.4	5	0.55	na	ns
Pacific wide	NO_x	Spearman r	-0.3	27	0.11	-0.63 to 0.09	ns
Marianas			0.3	9	0.36	na	ns
MHI			-0.3	7	0.44	na	ns
PRIAs			0.2	6	0.66	na	ns
Samoa			0.5	5	0.45	na	ns
Pacific wide	SiO_2	Spearman r	0.4	27	0.05	-0.01 to 0.67	ns
Marianas			-0.1	9	0.84	na	ns
MHI			0.4	7	0.44	na	ns
PRIAs			0.3	6	0.66	na	ns
Samoa			0.7	5	0.23	na	ns
Pacific wide	PO_4^{3-}	Spearman r	-0.3	27	0.19	-0.59 to 0.15	ns
Marianas			0.5	9	0.19	na	ns
MHI			-0.3	7	0.59	na	ns
PRIAs			0.1	6	0.92	na	ns
Samoa			0.6	5	0.35	na	ns

CHAPTER 4

Microbial-mediated Mechanisms of Reef Decline: A Review of the Current Literature

Abstract

Phase-shifts from coral to algal dominance are currently occurring on coral reefs world-wide. Although a number of anthropogenic pressures have been implicated, the mechanism(s) underlying these dramatic shifts in benthic community structure have yet to be revealed. The existing literature demonstrates a wide variety of potential mechanisms of reef-decline. In this review, we examine the current coral reef-literature on microbial-mediated mechanisms of reef-decline in relation to coral reef phase shift dynamics. By including new data from our own studies, we build on the DDAM hypothesis, the current model for how benthic reef algae overtake corals. In summary, we classify the ecological integrity of Pacific coral reef systems using a degradation threshold based on key macroecological patterns that emerged from our data analysis and propose a revised view of reef system degradation which includes the effects of human impact on microbial energy flux partitioning and the implications for reef resilience.

Introduction

In physics, a "phase transition" is characterized by "different patterns of qualitative behavior corresponding to different forms of internal organization separated by a sharp boundary" (1). For example, when liquid water freezes, cohesion forces dominate over thermal motion, and water molecules which were previously undergoing constant collisions with other molecules become locked into a regular lattice formation. In ecology, the terms "phase-shift" and "regime-shift" generally refer to a change in system-level behavior resulting from the crossing of a critical ecological threshold (2,3). In the case of water freezing, the system's "state" variables (variables used to describe the state of the system) include temperature, volume, and pressure. In most ecological systems where phase-shifts have been documented, the environment within which the system's state variables function changes in response to multiple human stressors and the system's state variables remain largely unknown.

Phase shifts on coral reefs: Coral reefs are unique systems in the sense that they are intensely competitive and dynamic environments when it comes to space on the substrate. The archetypal coral reef phase shift typically occurs as calcifyers (hard coral and crustose corraline algae) loose the battle to benthic algae, which include fleshy macroalgae (seaweed) or turf algae (a diverse assemblage of filamentous algae) (4-5). In the Caribbean, increased levels of anthropogenic disturbance have been shown to lead to macroalgal replacement of coral and/or CCA (6). In the Pacific, human impact typically leads to turf algal replacement of coral and/or CCA (7,8).

Coral disease outbreaks, fewer links in the trophic web, and loss of habitat complexity also occur in conjunction with anthropogenically-induced benthic phase shifts (9-11). Although a number of anthropogenic pressures have been implicated, including herbivore reduction due to overfishing and nutrient loading from pollution, the mechanistic cause of coral death remain a topic of debate (6, 12-14).

A growing body of evidence suggests that the combined effects of nutrient pollution and overfishing can initate microbially-mediated mechanism(s) by which turf algae gain a competitive advantage over corals. The DDAM (Dissolved organic carbon, Disease, Algae, and Microbes) model posits that when herbivorous fish and other grazers are removed from a coral reef, more fixed carbon from benthic primary producers becomes available to the reef-associated microbes (15-22). Turf algae are known to release large amounts of dissolved organic carbon (DOC) into the water column. A recent study by Haas et al. (2011) found that compared to CCA, scleractinian coral, and macroalgae, turf algae release the greatest amount of DOC per unit surface area (21). When percent cover data was considered, the amount of DOC predicted to be released by turf algae was still significantly higher even when coral, macroalgae, or CCA made up a greater percentage of substrate (Figure 4.1A; Kruskall-Wallis, $P < 0.0001$). For example, even on islands with relatively high calcifyer cover (50-60%) and low turf algae cover (15-20%), the amount of DOC predicted to be released by turf algae is roughly 2X higher than the amount of DOC

predicted to be released by calcifyers (~300 µmol hr^{-1} versus 150 µmol hr^{-1} $m^{-2,}$ respectively) (Figure 4.1B).

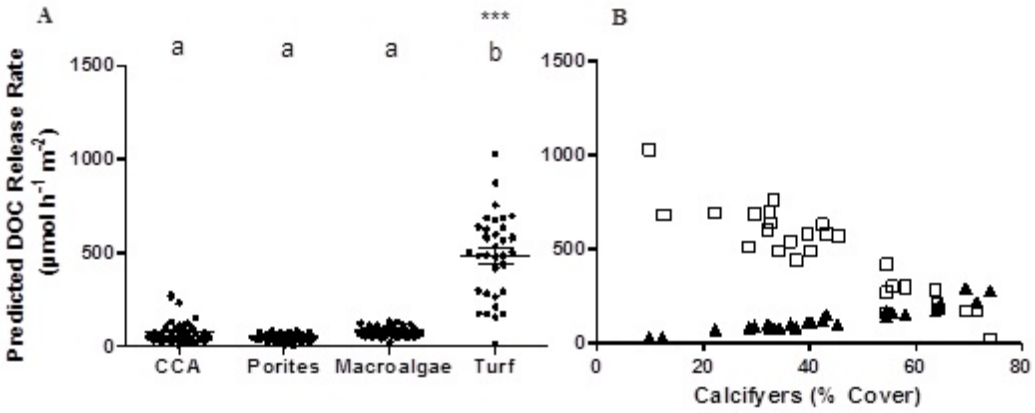

Figure 4.1A Box and whiskers plot of predicted DOC release rates for different benthic organisms for 29 Pacific Islands. Kruskall-Wallis followed by Dunn's multiple comparison found turf algae to be significantly different than CCA, Coral, and Macroalgae ($P<0.0001$). Figure 4.1B Relationship between the percent of the benthos occupied by calcifyers (hard coral and CCA) and the amount of DOC released by calcifyers (black triangles) versus turf algae (open squares) for the same set of islands.

DOC exuded from benthic reef algae may become a significant source of energy for heterotrophic microbes in human-impacted reef systems. In the same study, Haas et al. also showed that reef water associated microbes directly consumed DOC released by all four groups of benthic photosynthesizers (CCA, scleractinian coral, macroalgae, and turf algae) (2011).

Microbial-mediated mechanisms of coral death: The existing literature demonstrates a wide variety of microbially-mediated mechanisms of coral decline by

which turf algae could potentially gain a competitive advantage over corals and drive the system to an alternative stable state. The hypothesis that coral death is microbial-mediated was initially formulated in 2006 and is based on a combination of experiments published by Smith et al. and Kline et al (17-18). In the Smith et al. study, coral and algae were placed in the same chamber but separated by a 0.02 um filter, so that only dissolved compounds could pass between the coral and algae. Without antibiotics, 100% of the corals died; but when antibiotics were added to the chamber 100% of the corals survived. In the Kline et al. study, elevated levels of DOC (but not nitrate, phosphate, or ammonia) caused substantial coral mortality.

It is likely that microbially-mediated mechanisms of coral decline disrupt the balance between the coral and its associated *Bacteria* (22-24), the majority of which are related to known heterotrophs, thought to consume carbon-rich coral mucus (23, 25). As stated above, when herbivores lose control over the growth of benthic algae, an increased supply of algal-derived DOC (photosynthate) is released onto the reef. This DOC is a source of energy almost exclusively accessible to heterotrophic microbes (water column and/or surface-associated) many of which are opportunistic pathogens (microbes that are normally present within the environment but may opportunistically become causative agents of coral disease) (26). Disease outbreaks and coral death result in more free space available for DOC-producing fleshy algae. Increased microbial and viral loading with higher percentages of opportunistic and

specific microbial pathogens could potentially drive the system to an algal-dominated, alternative stable state.

This hypothesis is primarily supported by two key studies from Pacific island locations (26-27). In the first study, which included four coral atolls in the Line Islands, the proportion of microbial 16S rDNA sequences related to known pathogens was higher on reefs with the highest incidences of coral disease and the lowest percent coral cover (26). In the second study, Kelly et al. found that in regions of the Pacific where iron is limiting, corals were killed by reef rubble from shipwreck sites through microbial activity and that the microbial community became enriched in iron-associated virulence genes and known pathogens (2012). Phase shifts from calcifyers (coral and CCA) to turf algae also arose at shipwreck sites, most likely as a result of the microbial activity initiated by iron enrichment rather than DOC (27).

In comparison to coral-associated microbial communities, algal-associated microbial communities have been shown to harbor a higher percentage of autotrophs, which are less likely than heterotrophs to be opportunistic pathogens (23). However, coral mortality can also occur via pathogenic microbes vectored from benthic algae and algal-derived allelochemicals. There are instances in the literature when algae serve as reservoirs for coral pathogens (28-29). In the Caribbean, the macroalgae *Halimeda opuntia* has been shown to vector the bacterium *Aurantimonas coralicida*,

the causative agent of white plague type II, a disease that has caused widespread mortality in most Caribbean coral species (29).

In addition to pathogenic microbes, increased microbial respiration (resulting from increased rates of DOC consumption) can create hypoxic conditions at coral-algal interfaces and lead to hypoxia-induced mortality of coral tissue (22). In the 2006 study by Kline et al., elevated DOC levels accelerated the growth rate of microbes living in the corals' surface mucopolysaccharide layer by an order of magnitude (18). Whether hypoxia-induced mortality works in combination with other mechanisms of microbial pathogenesis remains an open question.

Other (non-microbial) processes that may facilitate coral to algal phase shifts: A number of studies have demonstrated that some macroalgae produce surface-associated metabolites that can directly poison corals at coral-algal interfaces; with damaging effects ranging from the inhibition of photosynthesis to tissue death (30-31). In addition, fleshy turf algal communities can trap sediment on coral reefs (even in cases where reef topography would otherwise facilitate transport of sediment down the reef slope onto the seafloor). A number of studies have shown that sediment load on reef substrata is negatively correlated with the percent cover of CCA (32-33). In a field study on Guam, Belliveau and Paul showed that herbivore exclusion cages had significantly increased sediment loads (2002). Therefore, in addition to preventing the initation of DOC-driven microbial-mediated mechanism of hard coral decline, it is

likely that herbivorous fish also play a role in directly mediating the competitive balance between CCA and turf algae.

Investigating the relationship between microbial energy flux and phase shifts: Although herbivore reduction due to overfishing probably facilitates coral to algal phase shifts, small increases in microbial biomass have a proportionately greater impact on the rate of energy transfer (W 10 m^{-3}) than large reductions in fish biomass (35). For example, roughly 1 gram of microbes uses approximately as much energy as 500 grams of fish (35). In a recent study by McDole et al., the microbialization of Pacific coral reefs (the process where energy and materials are redirected from macrobes to microbes; 36) was found to be strongly correlated with human impact; microbial metabolic rates were up to 100 fold higher on the most heavily impacted reef systems than on relatively pristine reef systems (35).

Building on the DDAM model: The findings described above are consistent with the DDAM model, where photosynthate fuels the growth of heterotrophic microbes (water column and/or surface-associated) (15). However, a large body of literature suggests that anthropogenic-based sources of nutrient input (i.e. agricultural run-off containing fertilizers and pesticides, untreated sewage, shipwrecks, etc.) also stimulate primary producers in both the water-column (phytoplankton) and the benthos (27-28, 34, 37-38).

In the open ocean and on coral reefs, heterotrophs dominate over autotrophs in terms of sheer microbial biomass (g 10 m^{-3}); however, because the average kinetic energy of activation is lower for photosynthesis than for respiration, microbial autotrophs dominate in terms of energy flux (W 10 m^{-3}) (39). In the open ocean there is a general trend towards increasing bacterial numbers and biomass with increasing primary productivity (40). On coral reefs, although the combined effects of overfishing and land-based pollution stimulate both groups of microbes, the relative fraction of autotrophs to heterotrophs has been shown to increase across increasing gradients of human activity (35, 39). This ultimately means that as a reef system becomes more and more impacted, the microbial community requires more energy, but becomes less efficient overall in terms of conversion of this energy into organic structure (Figure 4.4). This is because the resulting increase in energy use by the microbial community (microbialization) is primarily driven by autotrophic metabolism. Autotrophic microbes are much less likely to be potential pathogens, so partitioning less and less energy to heterotrophic microbes as human impact increases may dampen the negative effects of human activity by preventing the rise of pathogenic microbes, which would promote DDAM feedback and rapidly move the system towards an algal dominated state (39). It has been shown that continuous (as opposed to discontinuous) phase shifts may prevent hysteresis, making it easier for reef systems to return to “original” and/or less-degraded states (41). As anthropogenic stressors press state variables along a trajectory leading from one stable state to another (i.e. increased turf cover, reduced coral cover), the system may be less

vulnerable to DDAM feedback loop and hysteresis. It may be only in the severely degraded state (e.g., Christmas Atoll, Line Islands; 26) that relative competitiveness of autotrophic microbes becomes reduced, and the dominant controlling feedback shifts from autotroph-driven microbialization to heterotroph-driven DDAM feedback (where pathways of energy flow are reestablished through heterotrophic microbes with more pathogenic and/or copiotrophic growth strategies).

As previously stated, in most ecological systems where phase-shifts have been documented, the environment changes in response to multiple human stressors and little is known about how all of these processes interact to lead to phase-shifts and/or coral decline. Little progress has been made on identifying reliable indicators of coral reef function and resistance to perturbation (i.e. ecosystem state variables). In this study, we attempt to classify the ecological integrity of Pacific coral reef systems based on some key macroecological patterns that emerged from our data analysis which are interrelated by the theoretical framework presented above.

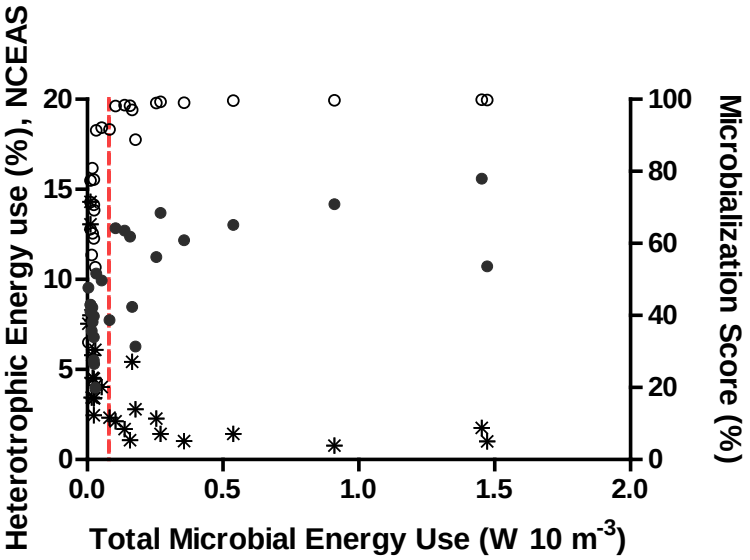

Figure 4.2 Relationships between total microbial energy use (x-axis) and three different indicators of reef decline. The three different island-level data sets are indicated by stars (the percent of total microbial energy use that is heterotrophic, left-axis), black circles (the NCEAS cumulative human impact score, left-axis) and open circles (the microbialization score, right axis). The dotted red line denotes a natural break in the data set of biological significance; it represents a threshold value beyond which total microbial energy use increases rapidly.

Figure 4.2 plots the relationship between total microbial energy use (heterotrophs + autotrophs) and three different indicators of reef decline. The dotted line shown on the x-axes represents a natural break in the data set that was identified using the Jenks Natural Breaks algorithm (a one dimensional clustering method where the variances within all classes are minimized while the variances among classes are maximized) (42). This break-point appears to be one of biological significance; it represents a threshold value beyond which total microbial energy use increases rapidly. This may be a degradation threshold, a point beyond which the state of the ecosystem begins to degrade but does not necessarily imply ecosystem collapse. For

this reason, we classify Pacific reef systems with total microbial energy use values below this threshold (0-0.08 W 10 m^{-3}) as “pristine”, while reefs above this threshold are classified as “intermediately” disturbed reefs (Figure 4.2). In general, the majority of human impact scores that occur beyond this break-point are relatively high (above a value of 10), microbialization scores are all above 80%, and the relative fraction of total microbial energy use required by the heterotrophic microbes decreases and remains low (below 2%). The benthic dynamics of the same set of Pacific reefs also appear to be related to increased microbial energy use (Figure 4.3a and b). In figure 4.3, a discontinuous increase in turf algal cover (>40%) and a sharp decrease in CCA cover (< 20%) both occur when total microbial energy use is above this break-point.

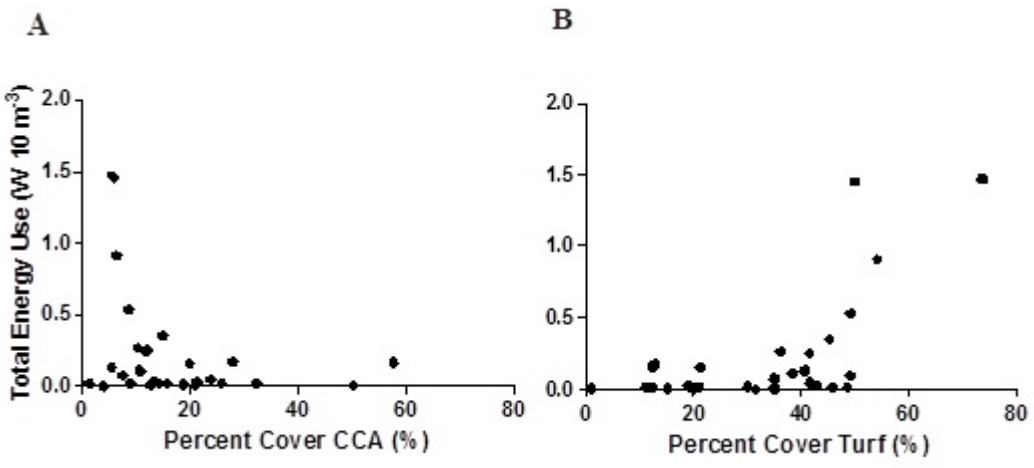

Figure 4.3 The relationship between island-level mean percent cover for a) CCA and b) turf algae and total predicted energy use by water-column associated microbes.

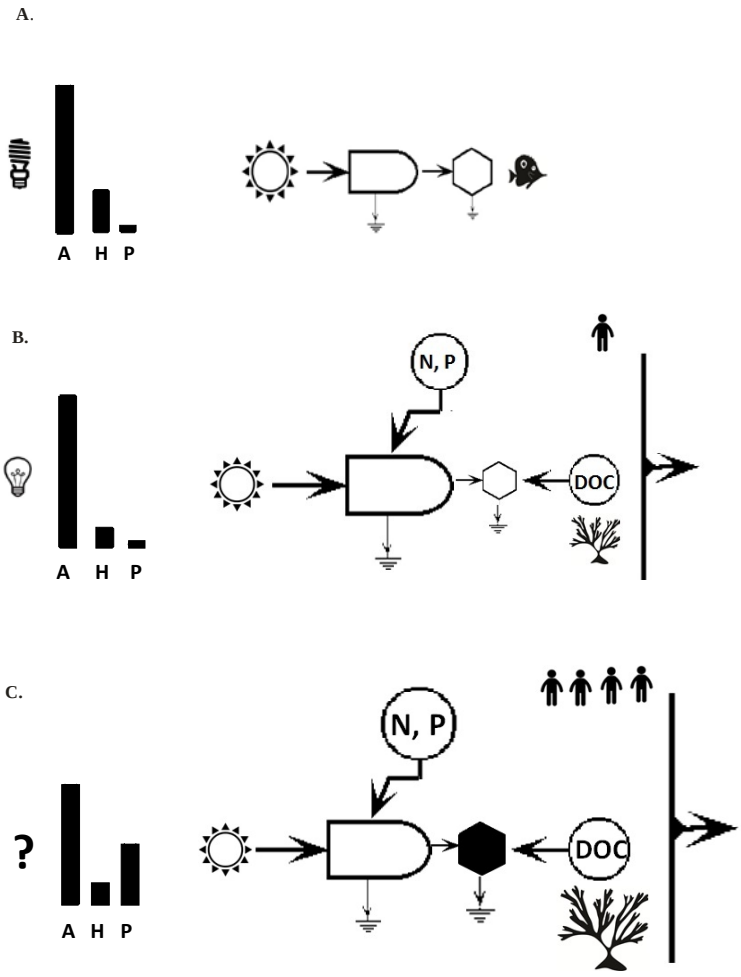

Figure 4.4 Changes in relative energy flux partitioning through microbial pathways in A. unimpacted Pacific reef systems, B. intermediately disturbed reef systems, and C. phase-shifted reef systems. In each state, bars represent the relative proportions of energy fluxed by autotrophic microbes (A), heterotrophic microbes (H), and opportunistic pathogens (P).The amount of energy fluxed by autotrophic microbes (rectangle with hemispherical cap), heterotrophic microbes (clear hexagon), and opportunistic pathogens (black hexagon) are generally scaled relative to each other to reflect the different contributions to total energy flux by each microbial group. These shapes can also be thought of in terms of energy circuit language (43). Important inflows of available energy are represented as circles with arrows and include: 1) solar radiation (sun icon), 2) nutrient loading (N, P), 3) algal derived photosynthate (algae icon, DOC). Concepts of system functioning represented as icons include: the importance of herbivorous fish in preventing algal growth (fish icon), increasing level of human activity (human icon), and changes in microbial energy efficiency (the amount of energy required per gram of microbial tissue) (light bulb). The vertical arrow to the right in B and C represent the large amount of energy dissipated as heat from the system

References

1. Solé, RV (2011) Phase Transitions. Princeton University Press, Princeton, NJ, USA.

2. Scheffer, M, Carpenter, S, Foley, JA, Folke, C and Walker, B (2001) Catastrophic shifts in ecosystems. Nature 413: 591–596.

3. Daskalov, GM, Grishin, AN, Rodionov, S and Mihneva, V (2007) Trophic cascades triggered by overfishing reveal possible mechanisms of ecosystem regime shifts. PNAS 104: 10518.

4. Barott, KL, et al. (2012) Natural history of coral−algae competition across a gradient of human activity in the Line Islands. Mar Ecol Prog Ser 460: 1–12.

5. Vermeij, MJA, Dailer, ML and Smith, CM (2011) Crustose coralline algae can suppress macroalgal growth and recruitment on Hawaiian coral reefs. Mar Ecol Prog Ser 422: 1–7.

6. Maliao, RJ, Turingan, RG and Lin, J (2008) Phase-shift in coral reef communities in the Florida Keys National Marine Sanctuary (FKNMS), USA. Mar Biol 154: 841–853.

7. Sandin, SA, et al. (2008) Baselines and degradation of coral reefs in the Northern Line Islands. PLoS ONE 3, e1548.

8. Bruno, JF, Sweatman, H, Precht, WF, Selig, ER and Schutte, VGW (2009) Assessing evidence of phase shifts from coral to macroalgal dominance on coral reefs. Ecol 90: 1478–1484.

9. Essington TE, Beaudreau AH, Wiedenmann J (2006) Fishing through marine food webs. Proc Natl Acad Sci USA 103: 3171-3175.

10. Greenstein BJ, Curran HA, Pandolfi JM (1998) Shifting ecological baselines and the demise of Acropora cervicornis in the western North Atlantic and Caribbean province: a Pleistocene perspective. Coral Reefs 17: 249-261.

11. McCormick M (1994) Comparison of field methods for measuring surface topography and their association with a tropical reef fish community. Mar Ecol Prog Ser 112: 87–96.

12. Szmant, AM (2002) Nutrient enrichment on coral reefs: Is it a major cause of coral reef decline? Estuaries 25: 743–766.

13. DeMartini EE, Friedlander AM, Sandin SA, Sala E (2008) Differences in fish-assemblage structure between fished and unfished atolls in the northern Line Islands, central Pacific. Mar Ecol Prog Ser 365: 199–215.

14. Vermeij, MJA, et al. (2010) The effects of nutrient enrichment and herbivore abundance on the ability of turf algae to overgrow coral in the Caribbean. PLoS ONE 5: e14312.

15. Dinsdale, EA and Rohwer, F (2011) Fish or germs? Microbial dynamics associated with changing trophic structures on coral reefs. Coral Reefs: An Ecosystem in Transition 231–240.

16. Vega Thurber, RL, et al. (2008) Metagenomic analysis indicates that stressors induce production of herpes-like viruses in the coral Porites compressa. Proc Natl Acad Sci U S A 105: 18413–18418.

17. Smith, JE, et al. (2006) Indirect effects of algae on coral: algae-mediated, microbe-induced coral mortality. Ecol Lett 9: 835–845.

18. Kline, D, Kuntz, N, Breitbart, M, Knowlton, N and Rohwer, F (2006) Role of elevated organic carbon levels and microbial activity in coral mortality. Mar Ecol Prog Ser 314: 119–125.

19. Wild, C, Niggl, W, Naumann, MS and Haas, AF (2010) Organic matter release by Red Sea coral reef organisms—potential effects on microbial activity and in situ O_2 availability. Mar Ecol Prog Ser 411: 61–71.

20. Haas, AF, et al. (2010) Organic matter release by coral reef associated benthic algae in the Northern Red Sea. J Exp Marine Biol and Ecol 389: 53–60.

21. Haas, AF, et al. (2011) Effects of coral reef benthic primary producers on dissolved organic carbon and microbial activity. PLoS ONE 6:11 e27973.

22. Barott, K, et al. (2009) Hyperspectral and physiological analyses of coral-algal interactions. PLoS ONE 4:11, e8043.

23. Barott, KL, et al. (2011) Microbial diversity associated with four functional groups of benthic reef algae and the reef-building coral Montastraea annularis. Environmental Microbiology 13: 1192–1204.

24. Bourne, DG, et al. (2009) Microbial disease and the coral holobiont. Trends Microbiol 17: 554-562.

25. Wild, C, et al. (2004) Coral mucus functions as an energy carrier and particle trap in the reef ecosystem. Nature 428: 66–70.

26. Dinsdale, E, et al. (2008) Microbial ecology of four coral atolls in the Northern Line Islands. PLoS One 3:2 e1584.

27. Kelly, LW, et al. (2012) Black reefs: iron-induced phase shifts on coral reefs. ISME J 6: 638–649.

28. Vega Thurber, R, et al. (2012) Macroalgae decrease growth and alter microbial community structure of the reef-building coral, Porites astreoides. PLoS ONE 7:9 e44246.

29. Nugues, MM, Smith, GW, van Hooidonk, RJ, Seabra, MI and Bak, RPM (2004) Algal contact as a trigger for coral disease. Ecol Lett 7:919–923.

30. Rasher, DB and Hay, ME (2010) Seaweed allelopathy degrades the resilience and function of coral reefs. Commun Integr Biol 3: 564–566.

31. Rasher, DB and Hay, ME (2010) Chemically rich seaweeds poison corals when not controlled by herbivores. PNAS 107: 9683–9688.

32. Purcell, SW (2000) Association of epilithic algae with sediment distribution on a windward reef in the northern Great Barrier Reef, Australia. Bull Mar Sci 66:199–214.

33. Fabricius, K and De'ath, G (2001) Environmental factors associated with the spatial distribution of crustose coralline algae on the Great Barrier Reef. Coral Reefs 19: 303–309.

34. Belliveau, SA, et al. (2002) Effects of herbivory and nutrients on the early colonization of crustose coralline and fleshy algae. Mar Ecol Prog Ser 232: 105–114.

35. McDole, T, et al. (2012) Assessing coral reefs on a Pacific-wide scale using the microbialization score. PLoS ONE 7:9 e43233.

36. Jackson, JBC, et al. (2001) Historical overfishing and the recent collapse of coastal ecosystems. Science 293: 629.

37. Pastorok, RA and Bilyard, GR (1985) Effects of sewage pollution on coral-reef communities. Mar Ecol Prog Ser 21: 175–189.

38. Brodie, J, Devlin, M, Haynes, D and Waterhouse, J (2011) Assessment of the eutrophication status of the Great Barrier Reef lagoon (Australia). Biogeochem 106: 281–302.

39. McDole, T, et al. submitted. Microbial-mediated resilience on intermediately disturbed coral reefs. Proc. R. Soc. B.

40. Azam, F, et al. (1983) The ecological role of water column microbes in the sea. Mar Ecol Prog Ser 10: 257–263.

41. Fung, T, Seymour, RM and Johnson, CR (2010) Alternative stable states and phase shifts in coral reefs under anthropogenic stress. Ecol 92: 967–982.

42. Jenks, GF (1967) The data model concept in statistical mapping, Int. Yearbook Cartogr. 7: 186–190.

43. Kubiszewski, I. and Cleveland, C. (eds) (2007) *Howard T. Odum energy circuit language* in: Encyclopedia of Earth. Washington, D.C.: Environmental Information Coalition, National Council for Science and the Environment.